AD-A131 837 STUDIES OF COLLISIONAL AND NONLINEAR RADIATIVE PROCESSES FOR DEVELOPMENT O..(U) ILLINOIS UNIV AT CHICAGO CIRCLE DEPT OF PHYSICS C K RHODES ET AL. 1/1

UNCLASSIFIED SEP 82 AFOSR-TR-83-0713 AFOSR-79-0130 F/G 20/14 NL

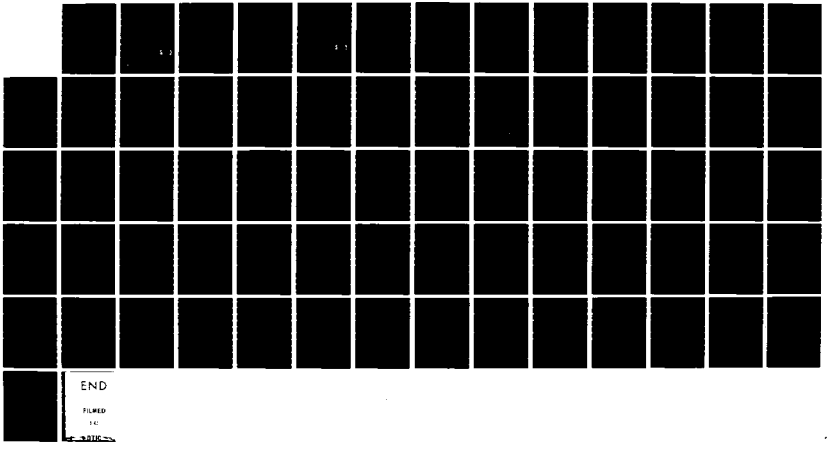

END

FILMED

DTIC

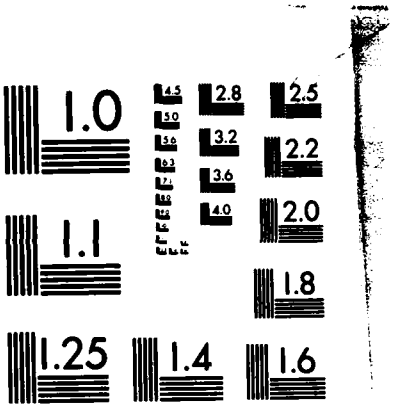

MICROCOPY RESOLUTION TEST CHART
NATIONAL BUREAU OF STANDARDS-1963-A

AD A131837

AFOSR-TR- 83-0713

"STUDIES OF COLLISIONAL AND NONLINEAR RADIATIVE PROCESSES FOR DEVELOPMENT OF COHERENT UV AND XUV SOURCES"

FINAL

~~Annual~~ Report

10/1/81 - 9/30/82

AFOSR-79-0130

DTIC
ELECTE
AUG 24 1983
A

DTIC FILE COPY

Approved for public release;
distribution unlimited.

83 08 19 102

UNCLASSIFIED
SECURITY CLASSIFICATION OF THIS PAGE (When Data Entered)

REPORT DOCUMENTATION PAGE

READ INSTRUCTIONS BEFORE COMPLETING FORM

1. REPORT NUMBER: AFOSR-TR- 83-0718	2. GOVT ACCESSION NO.: AD-A131 837
3. RECIPIENT'S CATALOG NUMBER:	
4. TITLE (and Subtitle): STUDIES OF COLLISIONAL AND NONLINEAR RADIATIVE PROCESSES FOR DEVELOPMENT OF COHERENT UV AND XUV SOURCES	5. TYPE OF REPORT & PERIOD COVERED: FINAL 1 Oct 81 - 30 Nov 82
	6. PERFORMING ORG. REPORT NUMBER:
7. AUTHOR(s): Charles K. Rhodes, Herbert Pummer, Hans Egger	8. CONTRACT OR GRANT NUMBER(s): AFOSR-79-0130
9. PERFORMING ORGANIZATION NAME AND ADDRESS: University of Illinois at Chicago, Department of Physics, Chicago, IL 60680	10. PROGRAM ELEMENT, PROJECT, TASK AREA & WORK UNIT NUMBERS: 61102F, 2301/A1
11. CONTROLLING OFFICE NAME AND ADDRESS: AFOSR/NP, Bolling AFB, Bldg #410, Wash DC 20332	12. REPORT DATE: Sep 82
	13. NUMBER OF PAGES: 65
14. MONITORING AGENCY NAME & ADDRESS(if different from Controlling Office)	15. SECURITY CLASS. (of this report): UNCLASSIFIED
	15a. DECLASSIFICATION/DOWNGRADING SCHEDULE

16. DISTRIBUTION STATEMENT (of this Report)

Approved for public release; distribution unlimited

17. DISTRIBUTION STATEMENT (of the abstract entered in Block 20, if different from Report)

18. SUPPLEMENTARY NOTES

19. KEY WORDS (Continue on reverse side if necessary and identify by block number)

20. ABSTRACT (Continue on reverse side if necessary and identify by block number)

High spectral brightness rare gas halogen (RGH) sources can be used to generate coherent extreme ultraviolet radiation by either harmonic generation mechanisms or direct multiquantum excitation of appropriate gain media. In order to demonstrate the basic characteristics of these two approaches, recent comparative measurements have been made. With the use of a 4 GW 193 nm (ArF*) system operating at a pulse duration of 10 ps, harmonic generation has been studied in several atomic and molecular media and used to generate 20 kW at 64.3 nm and 200 W at 38.6 nm. In addition, stimulated emission in molecular hydrogen, on

DD FORM 1 JAN 73 1473 EDITION OF 1 NOV 65 IS OBSOLETE

UNCLASSIFIED
SECURITY CLASSIFICATION OF THIS PAGE (When Data Entered)

20. Both the Lyman and Werner bands excited by two quantum absorption at 193 nm, has resulted in the generation of radiation as short as 117.6 nm at an efficiency of conversion approaching one percent. It has been concluded that the latter method is superior for the generation of short wavelength radiation. Extension of these results to both shorter wavelengths and higher power levels requires the ultraviolet. Recent studies of collision-free multiply-charged ion production with irradiation at 193 nm point to an anomalously strong coupling to high Z materials with processes involving as many as 99 quanta being observed. These multiquantum processes in the 40 - 80 eV range in certain atomic systems can be generated with existing laser instrumentation.

"STUDIES OF COLLISIONAL AND NONLINEAR
RADIATIVE PROCESSES FOR DEVELOPMENT
OF COHERENT UV AND XUV SOURCES"

FINAL

~~Annual~~ Report

10/1/81 - 9/30/82

AFOSR 79-0130

DTIC
ELECTE
AUG 2 4 1983
S
D
A

AIR FORCE OFFICE OF SCIENTIFIC RESEARCH (AFSC)
NOTICE OF TRANSMITTAL TO DTIC
This technical report has been reviewed and is
approved for public release IAW AFR 190-12.
Distribution is unlimited.
MATTHEW J. KERPER
Chief, Technical Information Division

University of Illinois at Chicago

College of Liberal Arts and Sciences
DEPARTMENT OF PHYSICS

Post Office Box 4348
Chicago, Illinois 60680
(312) 996-3400

ANNUAL REPORT
For the period 10/1/81 - 9/30/82

"STUDIES OF COLLISIONAL AND NONLINEAR RADIATIVE PROCESSES FOR DEVELOPMENT OF COHERENT UV AND XUV SOURCES"

by Charles K. Rhodes, Principal Investigator
Herbert Pummer, Co-Investigator
Hans Egger, Co-Investigator

Prepared for:

Dr. Barry Feldman
AFOSR/NP
Building 410, Room C219
Bolling Air Force Base
Washington, DC 20332

DTIC COPY INSPECTED

Accession For
NTIS GRA&I
Dist Special

ABSTRACT

High spectral brightness rare gas halogen (RGH) sources can be used to generate coherent extreme ultraviolet radiation by either harmonic generation mechanisms or direct multiquantum excitation of appropriate gain media. In order to demonstrate the basic characteristics of these two approaches, recent comparative measurements have been made. With the use of a 4 GW 193 nm (ArF*) system operating at a pulse duration of $\sim$ 10 ps, harmonic generation has been studied in several atomic and molecular media and used to generate $\sim$ 20 kW at 64.3 nm and $\sim$ 200 W at 38.6 nm. In addition, stimulated emission in molecular hydrogen, on both the Lyman and Werner bands excited by two quantum absorption at 193 nm, has resulted in the generation of radiation as short as 117.6 nm at an efficiency of conversion approaching one percent. It has been concluded that the latter method is superior for the generation of short wavelength radiation. Extension of these results to both shorter wavelengths and higher power levels requires an extended study of the basic character of high order nonlinear processes in the ultraviolet. Recent studies of collision-free multiply-charged ion production with irradiation at 193 nm point to an anomalously strong coupling to high Z materials with processes involving as many as 99 quanta being observed. These findings strongly suggest that the direct excitation of inversions by appropriate multiquantum processes in the 40-80 eV range in certain atomic systems can be generated with existing laser instrumentation.

CONTENTS

I. INTRODUCTION

Recent experimental studies show that bright tunable radiation in the 10 nm to 100 nm spectral range can be generated with the use of high brightness rare gas halogen (RGH) laser systems. Fundamentally, this approach is predicated on the extraordinary advances made in the spectral brightness of RGH media in recent times.[1-5]

Since nonlinear coupling is common to all processes involving frequency up-conversion of RGH radiation, a premium value is placed on the ability to produce outputs of maximal power and intensity. For this elementary reason, current experimental efforts are concentrating on the understanding and use of spectrally bright picosecond RGH systems. Presently, an instrument developing a power of 4 GW at 193 nm (ArF*) is being used in the examination of physical processes suitable for wavelength conversion to the vacuum ultraviolet (VUV) and extreme ultraviolet (XUV) ranges.

This report concerns the physical studies which we feel will lead to genuine stimulated emission in the soft x-ray range at quantum energies in the 40-80 eV region. The basic conclusion that a source of this nature is now feasible with existing instrumentation is supported by (1) the favorable scaling relationships governing RGH technology and (2) an accumulating body of evidence demonstrating the efficacy of nonlinear processes for the selective production of high lying atomic states. If the inferences from currently available information have been correctly drawn, their principal implication is the feasibility of a relatively modest laboratory scale x-ray laser operating at a wavelength of $\sim$ 1 nm.

II. APPLICATIONS TO BASIC PHYSICAL MEASUREMENTS

The availability of bright XUV and soft x-ray radiation will have important ramifications for a broad range of basic physical studies over the next few years. Certainly, one of the most significant would be the construction of a microhologram of living matter,[6] a technique of measurement that could become a routine biological assay, if a coherent source of 1 nm radiation were available. However, for illustration here, two other areas of application, one involving inertial fusion plasma diagnostics and the other concerning condensed matter surface studies, are outlined below.

A. Inertial Fusion Plasma Diagnostics

Diagnostic techniques useful for hot, dense, and small plasmas are crucial for the evaluation of inertial-confinement fusion.[7] Currently, pulsed x-ray shadowgraphy has been performed[8] only under conditions for which the laser energy used to provide the diagnostic x-ray source, from a separate laser plasma, was comparable to that used to illuminate the target of interest. This condition arises, since the x-ray source must irradiate the film with a flux at least comparable to the intense x-radiation originating from the target in order to produce a useful shadowgraph exposure. Interferometric applications place an additional bandwidth requirement on the x-ray source, since the coherence length must be comparable to or greater than the physical dimensions of the plasma.

The combination of narrow spectral bandwidth and spatial coherence very greatly reduces the x-ray power needed under experimental circumstances typical of current inertial confinement fusion studies. An estimate[9] of the minimum x-ray power required from the diagnostic source for a shadowgraph study concludes that a total power of ∿ 10-100 kW at 19.5 nm is sufficient to perform coronal studies of a target having a radius of ∿ 100 μm and a temperature of 3 KeV. In order to provide a sharp spectral filter at 19.5 nm, the wavelength is selected to match the narrow minimum that exists in the absorption to an autoionizing (sp 23+) $^1P^o$ level in neutral helium.[10] This absorption profile at 63.6 eV, taken from the previous work of Madden and Codling,[10] is shown in Fig. (1). The narrow minimum is the significant feature which, in the case of a single discrete state interacting with a single continuum,[11] with neglect of the very small influence of the Doppler effect, will represent an absorption that vanishes exactly. Examination of the 2s2p $^1P^o$ resonance at ∿ 60.1 eV in helium indicates a minimum experimentally consistent with zero; the (sp, 23+) $^1P^o$ resonance shown in Fig. (1), since it is narrower, is affected by instrumental resolution. Since the medium is transparent for a small range $\Delta\lambda$ about the wavelength of a minimum absorption, although opaque elsewhere, this effect provides a very high resolution filtering function. Straightforward analysis utilizing the narrow spectral width represented by the helium filter and spatial coherence available leads to the conclusion that a total power in the 10-100 kW range is sufficient for the performance of coronal studies. Indeed, with the use of a streak camera, an x-ray movie of an implosion could be generated by using a staggered set of picosecond XUV pulses.

B. Condensed Matter Surface Studies

Bright sources of coherent XUV or soft x-ray radiation can greatly facilitate surface studies of condensed matter. Indeed, it appears possible to provide a rate of measurement sufficiently high to permit picosecond time scale resolution of the dynamics of surface morphology on the atomic scale.[5] As an example of the diagnostic capability that can be achieved, an analysis of time-resolved photoemission studies[5] concludes that the detailed behavior of the recrystallization of laser annealed semiconductors could be recorded with pulses of ∿ 10 ps duration at a power of ∿ 100 kW. Since growth velocities of 2-5 m/sec are believed to be generally characteristic[12] of the recrystallization rate of annealed material, a time resolution of ∿ 10 ps is sufficient to observe the regrowth of a single atomic layer. We note that a power of 20 kW at 64.4 nm (19.3 eV) in 10 ps pulses has been reported in preliminary experiments examining harmonic generation, a result contained in Table I below.

III. PICOSECOND 193 nm SOURCE

The basic 4 GW system, with a pulse duration of 10 ps and spatial and spectral properties close to their respective transform limits, is illustrated in Fig. (2). In the configuration shown, the output of a synchronously pumped, mode-locked dye laser (Coherent Radiation 599-04, λ = 580 nm, pulse duration ∿ 8 ps) is pulsed amplified in a three-stage, XeF* excimer laser pumped dye amplifier. The amplified spontaneous emission arising from the dye amplifiers is suppressed by two 250 μm thick saturable absorber cells which are installed between the consecutive amplifier stages. The most stable operation of the amplifier chain has been achieved with DQOCI (1×10^{-3} mol/ℓ in methanol) as the saturable absorber. Besides DQOCI, DODCI and malachite green have been tested in different solvents. Under typical conditions, the 580 nm output pulse has an energy of ∿ 1 mJ.

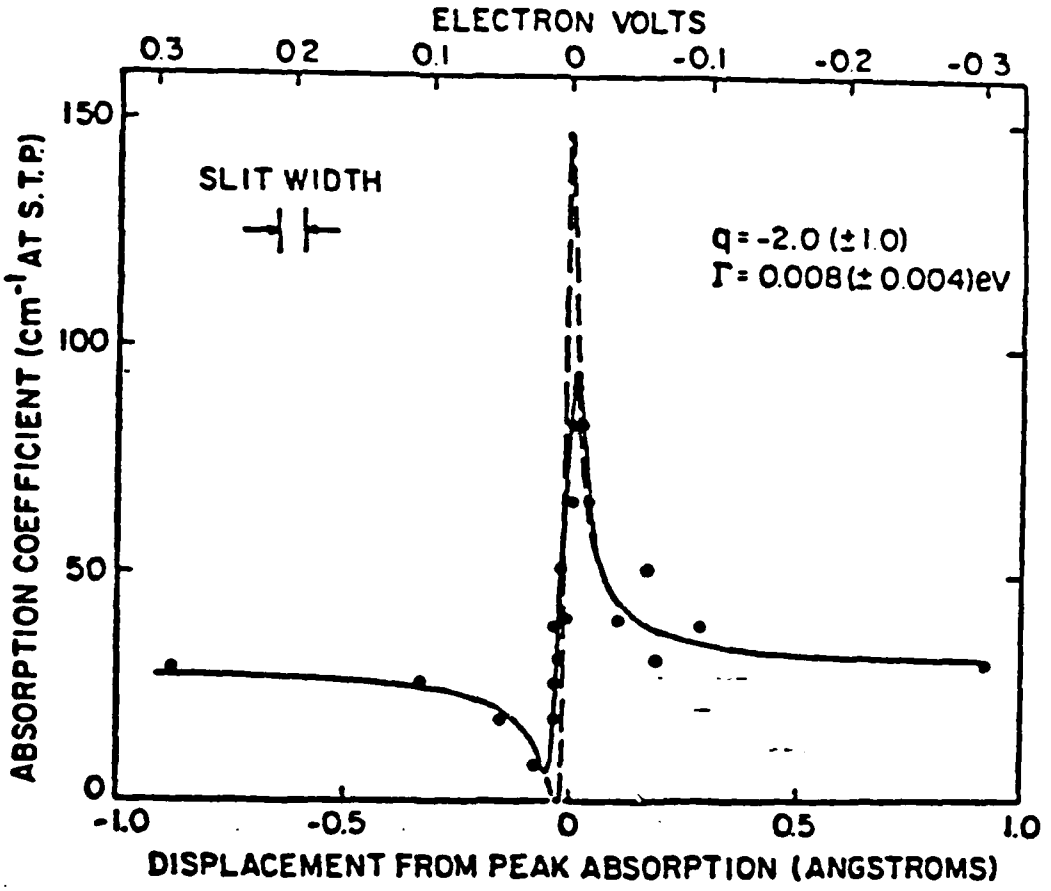

Fig. (1): Absorption profile of neutral helium at 63.6 eV according to the data of Madden and Codling (ref. 10). The dashed curve indicates true atomic response with compensation for instrumental resolution.

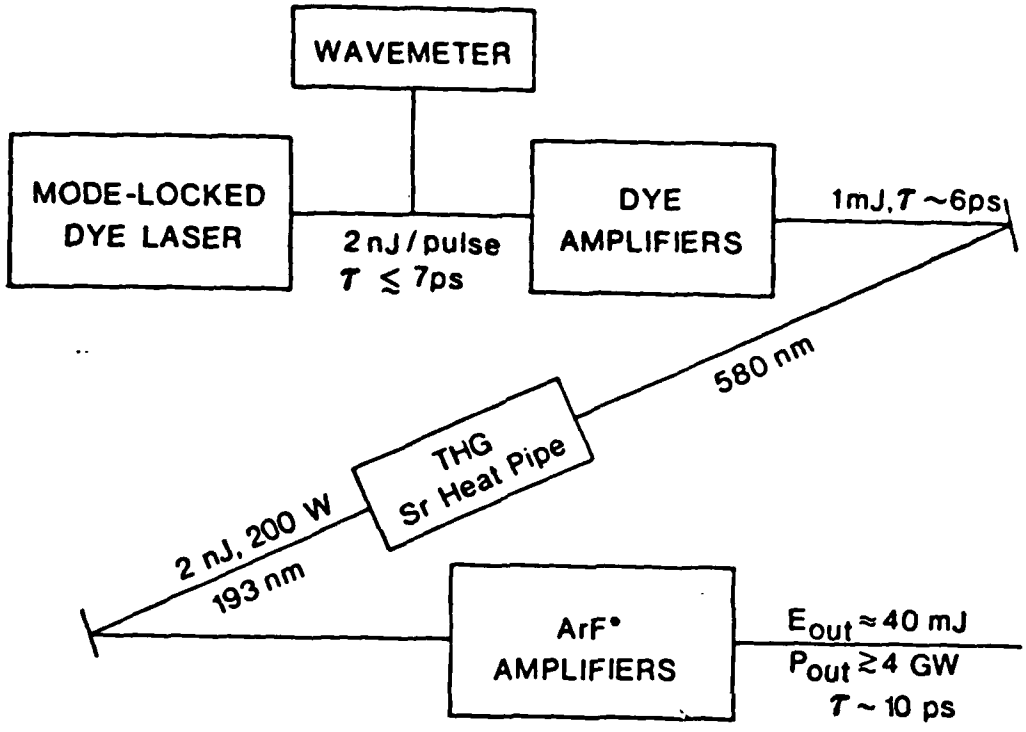

Fig. (2): Schematic diagram of 10 picosecond 193 nm (ArF*) system showing characteristic energy, pulse duration, and power levels.

The 1-mJ, 580-nm output pulse is focussed with a 35-cm focal-length lens (f/50) into a strontium heat pipe, in which ∿ 2 nJ of the third harmonic at 193 nm is produced. Subsequently, the 2 nJ, 193 nm output from the heat pipe is initially amplified in a double-pass ArF* amplifier. A spatial filter and a grating-pinhole combination with a 25 cm^{-1} bandpass is used to suppress amplified spontaneous ArF* emission. After further amplification in a single-pass amplifier, the energy in the short pulse is typically 5 mJ with an additional 5 mJ contained in amplified spontaneous emission. When this pulse is focussed with a 20 cm focal length lens, an air breakdown is readily observed. After final amplification in a second single pass amplifier, 30 ± 10 mJ are typically measured in the short pulse and ∿ 200 mJ in the amplified spontaneous emission. It is important to note that the short pulse energy observed represents a substantial fraction of the maximum energy available for extraction (∿ 50 mJ) in a pulse shorter than the excimer lifetime. This level of extraction is direct evidence against the presence of a significant nonlinear loss mechanism affecting the amplification of the picosecond pulse up to an intensity of ∿ 1 GW/cm^2. The duration of this final output pulse is determined to be ∿ 10 ps, as shown in Fig. (3).

In addition to the temporal behavior of the ArF* pulse, the coherence properties of the beam have been studied and compared to those of the 580 nm visible beam. In both cases, interference fringes were visible up to a maximum delay of ± 3 ps, indicating comparable coherence lengths for both the visible and ultraviolet pulses. A magnitude of ∿ 5 cm^{-1} has also been derived from the observation[13] of a two quantum resonance[14] in the X→E,F band of H_2, a value consistent with the fringe determination. Correspondingly, the bandwidth of the 193 nm pulse is estimated to be ∿ 5 cm^{-1}.

IV. HARMONIC GENERATION

Naturally, the high intensities available with the 10 ps output favor the observation of nonlinear processes. Therefore, harmonic generation in gaseous media serves as a simple and effective means for the production of radiation in the range below 100 nm. Preliminary experiments examining the nonlinear scattering in various gases such as H_2, He, Ne, Ar, N_2, and CO indicate substantial production of both third (64 nm) and fifth (39 nm) harmonic radiation. Table I summarizes the results obtained in these early measurements. The maximum powers observed at the third harmonic (64 nm) and the fifth harmonic (39 nm) were ∿ 20 kW and 200 W, respectively.

TABLE I. Harmonic generation with 193 nm, 10 ps pulses.

	XUV POWER (W)	
Gas	3rd harmonic	5th harmonic
H_2	2×10^4	∿2
He	20	2
Ne	20	20
Ar	2×10^4	200
N_2	200	20
CO	20	0

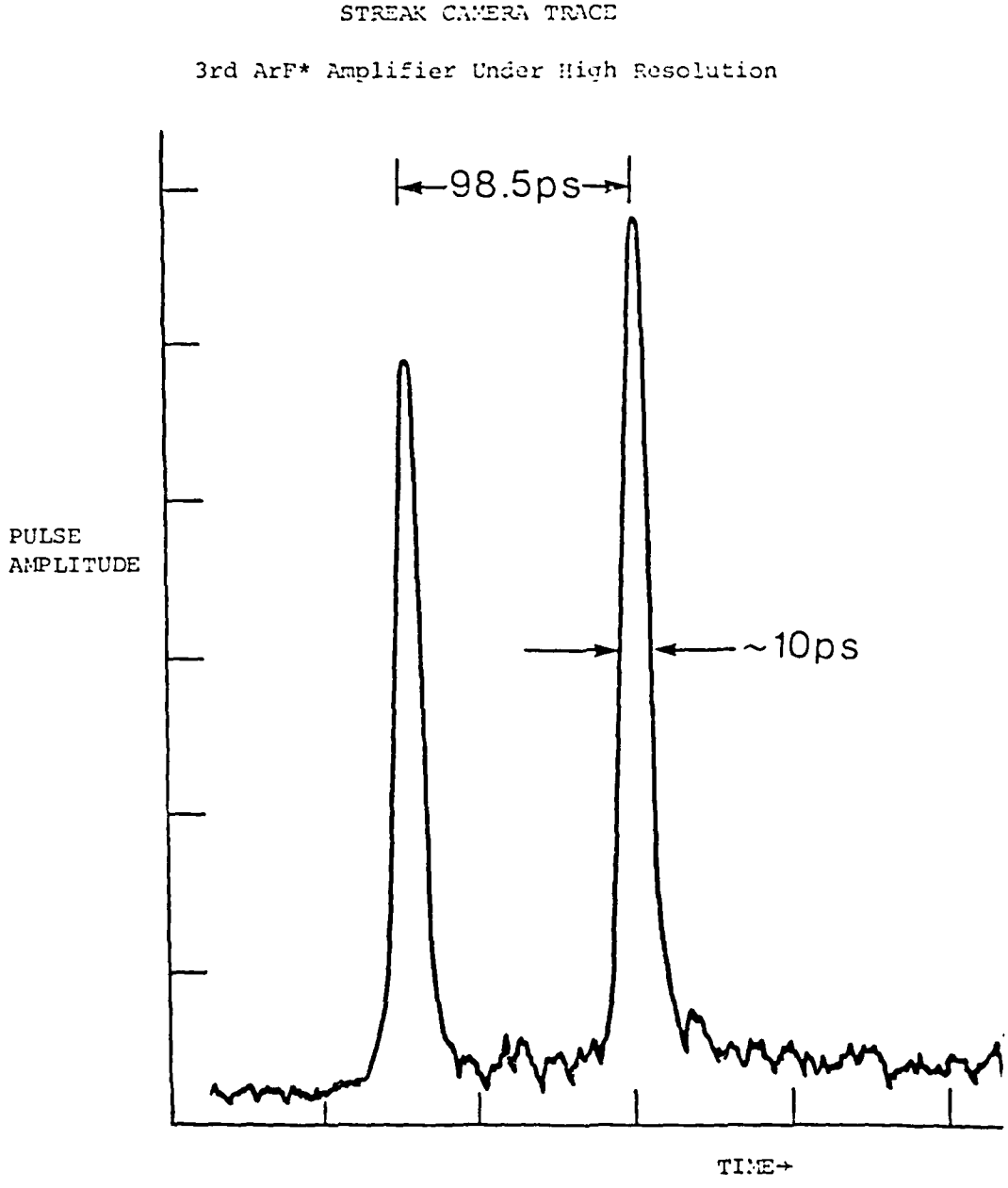

Fig. (3): Streak camera recording of ArF* laser emission after the final amplifier at high temporal resolution showing actual pulse duration. The two pulses are the front and rear surface reflections from a 9.5 mm quartz flat which was used to calibrate the time axis.

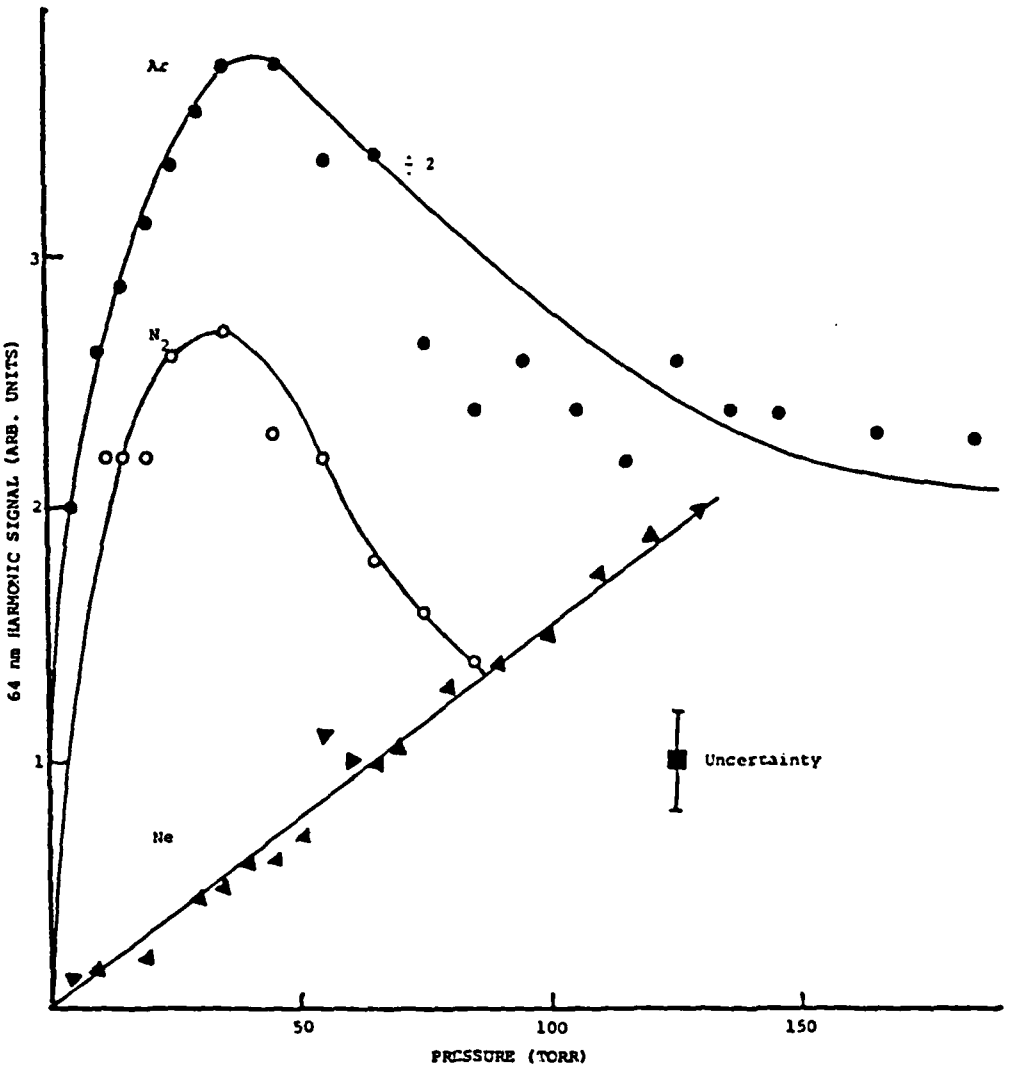

Fig. (4): Intensity of third harmonic (64 nm) signal as a function of medium density using 10 psec 193 nm radiation.

The density dependence of the nonlinear intensity is revealing. All neutral gaseous materials, with the exception of He and Ne, will present a loss at 64 nm arising from photoionization. The presence of this loss, for a given focal geometry, establishes a fundamental upper limit on the density of the nonlinear medium for optimum conversion. As shown in Fig. (4), N_2 and Ar both exhibit diminishing 64 nm output as densities above $\sim 1.5 \times 10^{18}$ cm^{-3} as a consequence of the absorption from photoionization. However, since the losses arising from photoionization at 64 nm in neon are totally absent, a different behavior is seen. Pressure-induced absorption[15] at 64 nm will occur at sufficiently high density in a manner similar to that observed in krypton, as well as many other materials, but this is not expected to be an appreciable effect for densities less than $\sim 2 \times 10^{20}$ cm^{-3}. With the use of a high pressure pulsed valve for the production

of the nonlinear medium, the scaling behavior indicated for neon in Fig. (4) implies the generation of XUV power levels in the megawatt range.

V. STIMULATED EMISSION FROM MULTIPHOTON EXCITED INVERSIONS

Direct radiative excitation by multiquantum processes can be used to generate amplification in the XUV and soft x-ray regions. It is apparent from the comparison of the properties of direct stimulated emission with those of parametric processes, such as harmonic generation, that the former will provide the most efficient mechanism for conversion to the soft x-ray region. Multiquantum processes of this nature, which have previously been observed in the infrared,[16] can now be readily extended to the shorter wavelength region with high spectral brightness picosecond RGH sources.

Molecular hydrogen represents the essential paradigm of this basic mechanism in the VUV range. The previously[14] studied $X\ ^1\Sigma_g^+ \rightarrow E,F\ ^1\Sigma_g^+$ Q(2) transition in H_2 falls in a region in which exact resonance can be achieved for an allowed two quantum excitation with 193 nm radiation. For irradiation with 10 ps pulses, estimates indicate that approximately one percent of the H_2 ground state population can be transferred to the excited state at an intensity of $\sim 10^{11}$ W/cm^2 when proper account is made for losses due to photoionization of the $E,F\ ^1\Sigma_g^+$ level at 193 nm. Therefore, at a medium density of 2×10^{19} cm^{-3}, with an allowance for rotational partition, an inversion density of $\sim 10^{17}$ cm^{-3} on the $E,F\ ^1\Sigma_g^+ \rightarrow B\ ^1\Sigma_u^+$ can be generated. Since the cross section for the E↦B transition $\sigma_{EB} \cong 6 \times 10^{-14}$ cm^2, an enormous gain constant $g_{EB} \sim 6 \times 10^3$ cm^{-1} is obtained, and strong stimulated emission on the relevant transitions in the near infrared from 750 nm to 920 nm is observed. As a direct consequence of the E↦B emission, the B↦X molecular Lyman transition develops an inversion of comparable magnitude which, together with the cross section for the B↦X transitions, will exhibit a gain $g_{BX} \sim 10^3$ cm^{-1}. An amplification of this magnitude will lead to saturation in a distance of less than 1 mm. Naturally, this leads to the observation of intense stimulated emission[17] on the Lyman band in the 127 nm - 155 nm region. The shortest wavelength observed in this manner on the Lyman band was ∿ 127 nm corresponding to the (0-3) transition. The cascading stimulated transitions producing the Lyman $(1,\nu)$ bands are illustrated in Fig. (5). Most significantly, we note that the conversion efficiency from the 193 nm radiation to the up-converted light was determined to be ∿ 0.5% for a <u>single</u> rotational transition. Assuming that the VUV pulses occur on a time scale of ∿ 10 ps, the signal strength observed indicated a peak power on the strongest transition of ∿ 20 MW. In addition, strong stimulated emission has also been observed on the Werner $C\ ^1\Pi_u \rightarrow X\ ^1\Sigma_g^+$ band at 117.6 nm corresponding to the (2,5) transition. Characteristic stimulated spectra illustrating the observed B↦X bands ∿ 154 nm and the 117 nm C↦X transition are shown in Fig. (6) and Fig. (7), respectively. A more detailed discussion of this system, including the role of the optical Stark effect, is contained in Appendix A.

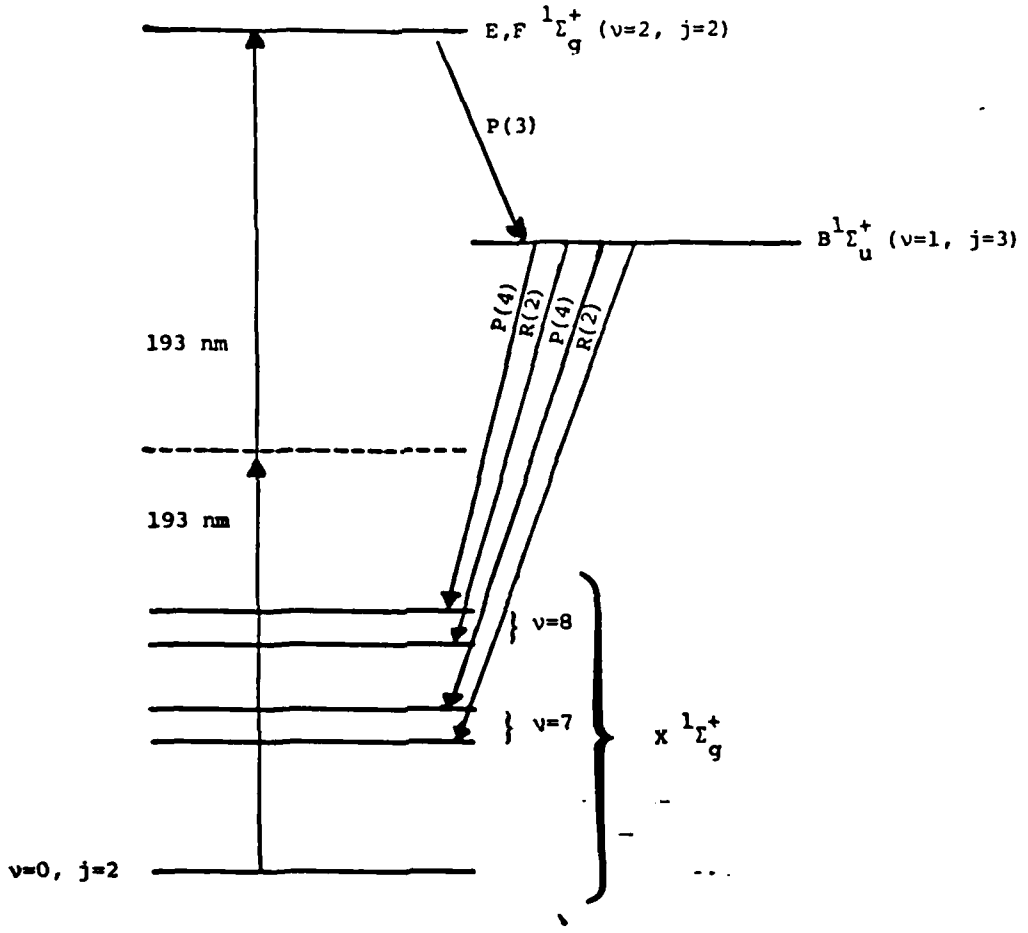

VUV Stimulated Emission Wavelengths (nm)

B→X	1-6	1-7	1-8
P(4)	144.1	150.0	155.8
R(2)	142.9	148.8	154.6

Fig. (5): Partial energy level diagram for hydrogen, illustrating the two-photon excitation with subsequent stimulated emission in the infrared and the vacuum ultraviolet involving the Lyman (1,v) band.

Fig. (6): Hydrogen B→X bands observed in stimulated emission with two quantum excitation at 193 nm arising from Q(2) and Q(3) excitation.

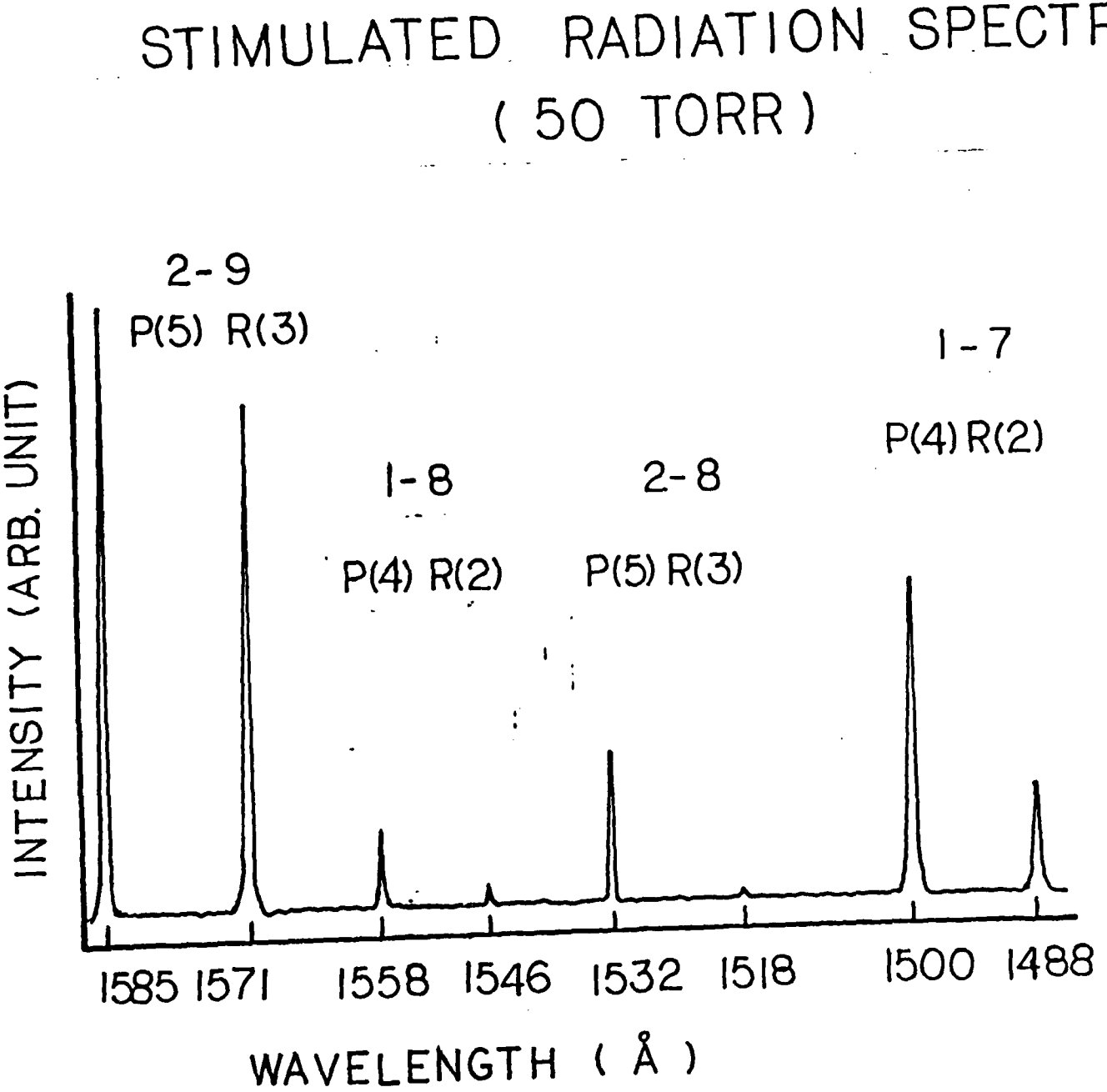

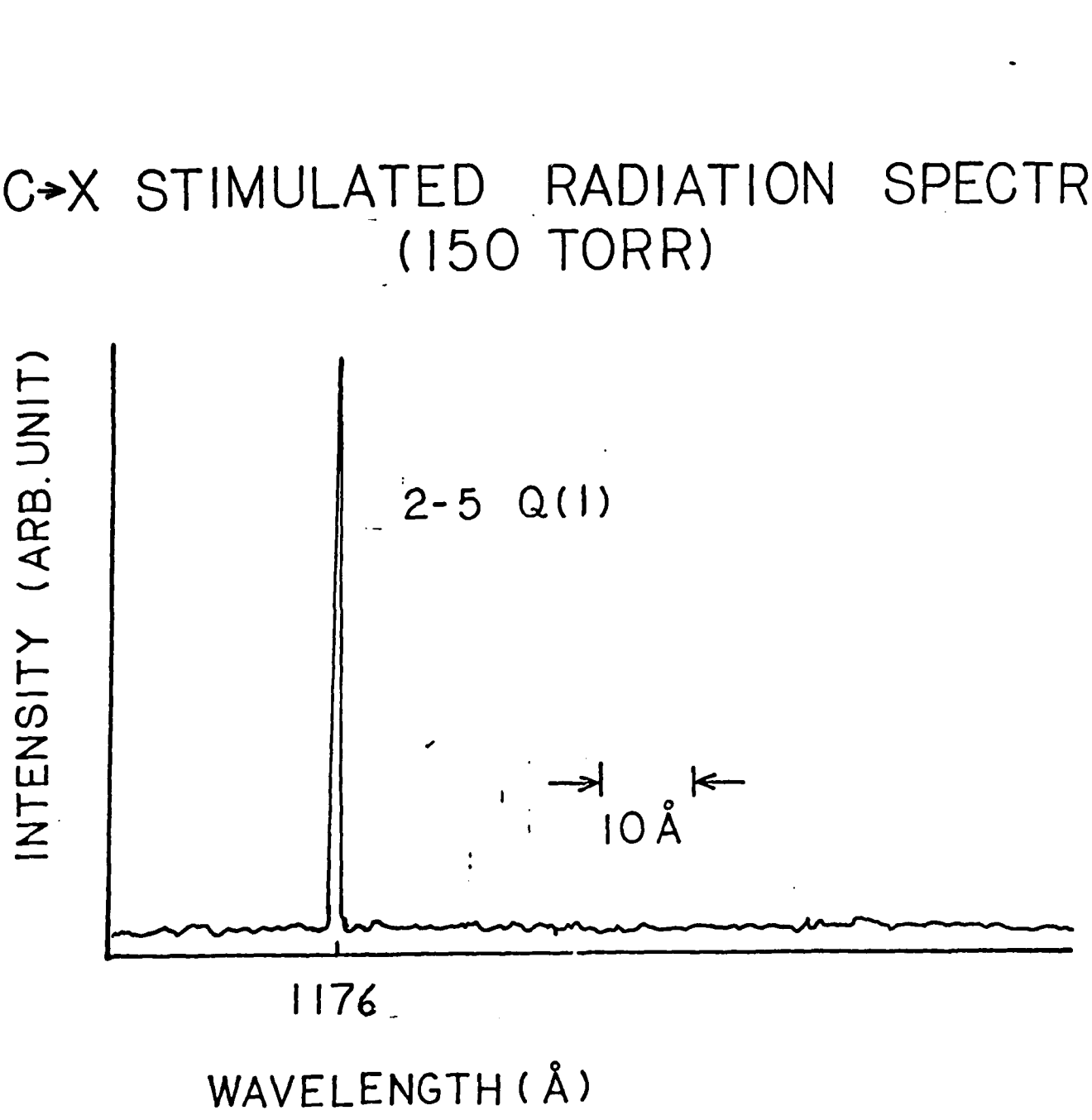

Fig. (7): Hydrogen C→X transition observed in stimulated emission with two quantum excitation at 193 nm arising from Q(2) excitation.

VI. STUDY OF THE MECHANISM FOR THE PRODUCTION OF MULTIPLY CHARGED IONS

Multiply charged ions of krypton have been produced[18] under collision-free conditions with 1.06 μm radiation at relatively low intensity, less than 10^{14} W/cm^2. These results suggest the possibility of direct selective population of high lying states by a multiquantum process involving a large number of quanta. Indeed, it is possible to speculate on the possible role of a collective atomic response of the type described by Wendin.[19] Naturally, the large matrix elements that might arise in this fashion would have a very substantial influence on a high order multiquantum process. Furthermore, these factors may be substantially modified by recently reported intensity dependent effects on configuration interaction.[20]

Presently, we have begun operation of an atomic beam apparatus for use in conjunction with the 193 nm source described in Section III. This apparatus is equipped with an electrostatic analyzer so that individual charge and mass states can be readily observed. A simple demonstration of the ion detection capability is shown in Fig. (8) which displays the H^+ and H_2^+ peaks generated by illumination of H_2 at 193 nm. The intensity dependence[21] of these ion signals strongly indicates that the H^+ production arises from secondary photolysis of H_2^+.

Preliminary results indicating the formation of multiply charged ions with 193 nm irradiation, spanning the range in atomic number[22] from He to U, have also been obtained. The results of these studies are contained in Appendix B. These results were obtained at a rather low intensity, $\lesssim 10^{14}$ W/cm^2, not far from the range studied by L'Huillier et al.[18]

The principal findings of the results discussed in Appendix B are (1) the unexpectedly strong multiphoton coupling strength resulting in multiple ionization of target atoms, (2) a strong Z-dependence of the coupling, and (3) ion charge state distributions which in some cases resemble those characteristic of Auger cascades. Conventional stepwise models of sequential ionization using standard theoretical techniques are found to be wholly incapable of describing these results. To unify these experimental findings within the framework of a single physical picture, a mode of interaction which involves direct radiative coupling to a collective motion of an inner-shell with subsequent transfer of excitation to a corresponding outer-shell is proposed.

Fig. (9) illustrates the atomic number dependence of the total energy transferred as represented by the maximum charge state observed. A substantial increase in coupling is evident for the heavier materials. We note that the overall shape of the envelope curve suggests a change in the basic coupling mechanism as the atomic number increases. The anomalous magnitude of the coupling strength at high Z points strongly to a collective mode[23] of excitation. Some aspects of these findings are discussed in Appendix B.

Certainly more detailed physical measurements are required to (1) clarify the mechanisms which give rise to the observed response and (2) to demonstrate the selectivity expected for the production of certain ionic excited states. In this we are mindful of strong dynamical effects, such as f-electron collapse,[24,25] which may influence the coupling. For the examination of these questions we intend to measure both the electron spectra and photon spectra arising from the excited material. The current apparatus, operating at $\sim 10^{-6}$ Torr, can be used to determine the electron distribution. For the study of photon emission, a modification

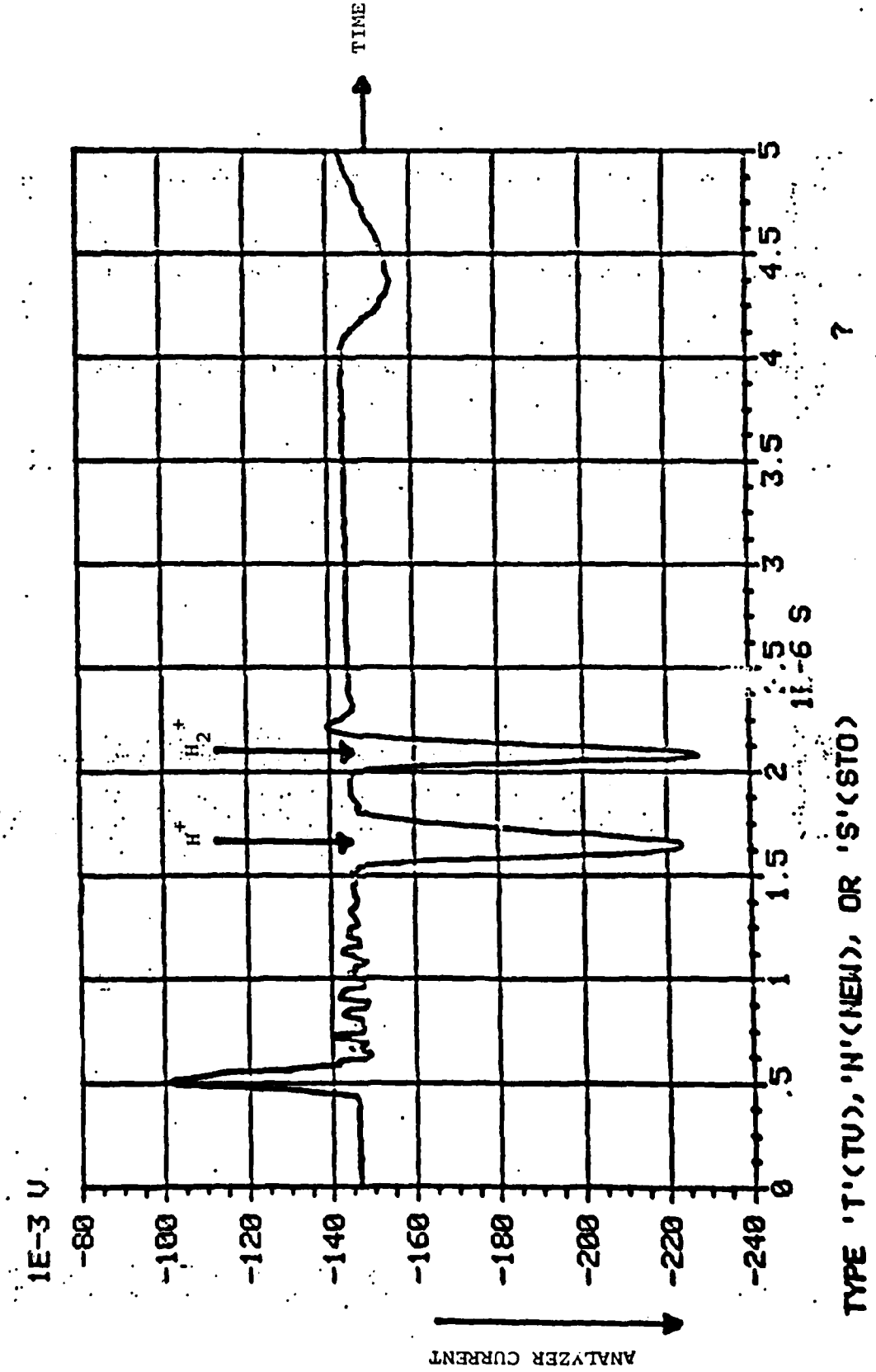

Fig. (8): H_2 ion spectra; H_2 irradiated at 193 nm shown time of flight analysis of proton and H_2^+ formation.

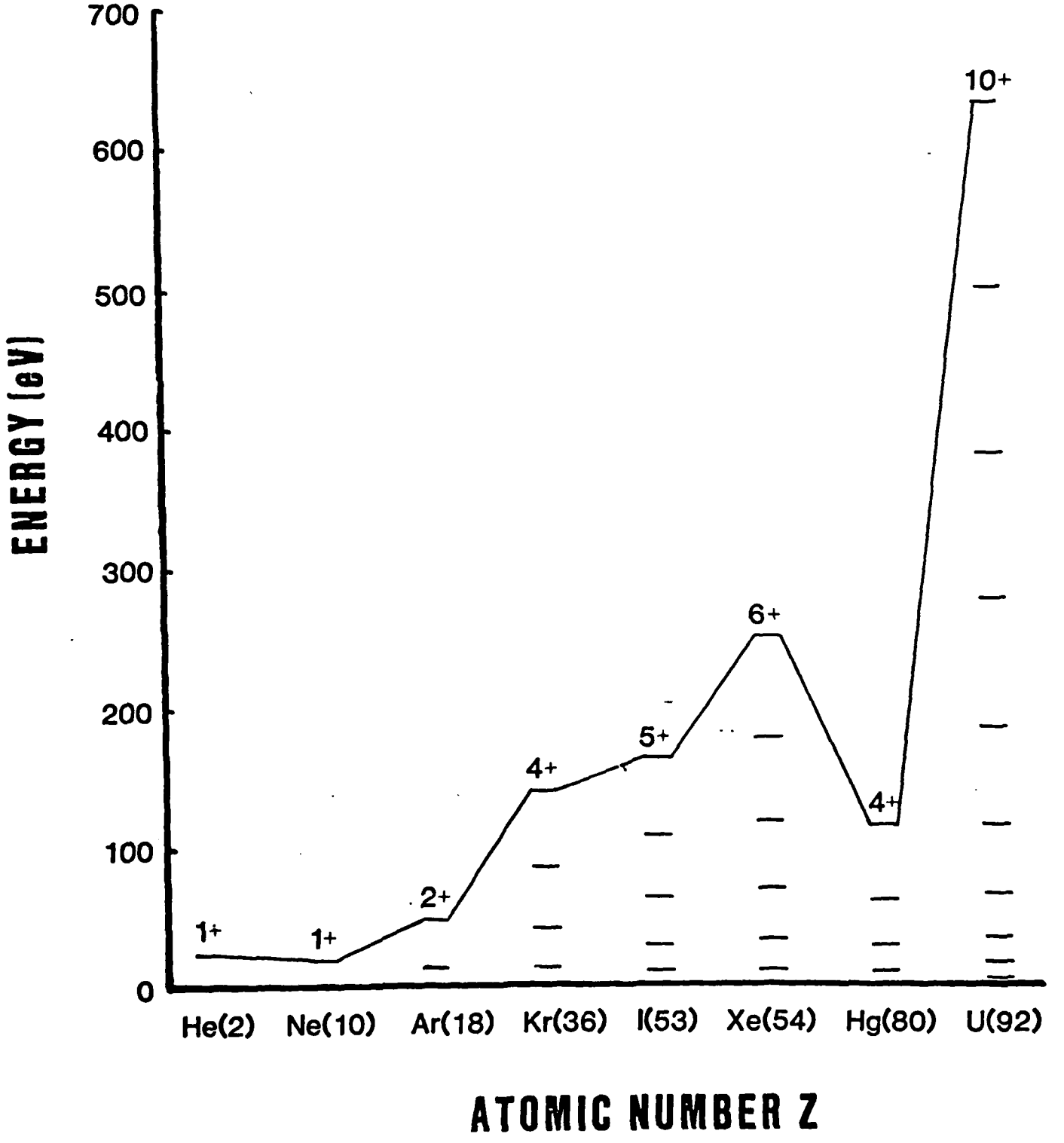

Fig. (9): Plot of the ionization energies representing the total energy transfer required for the production of different charge states as a function of atomic number (Z). The envelope curve is drawn to connect the states representing the maximum charge state observed.

involving a pulsed jet will be necessary to raise the density in the experimental volume.

VII. CONCLUSIONS

The development of excimer laser systems during the last decade has culminated in the availability of a new and extremely power light source technology in the ultraviolet region. Clearly, the extremely high brightness available from RGH technology has important implications for the production of bright, coherent radiation in the XUV and soft x-ray regions. A review of the scaling properties of RGH media leads to the conclusion that modest laboratory scale systems can be implemented at the $\sim$ 1 TW power level. This should enable the production of bright sources of coherent radiation in the 10^2-10^3 eV range. Such sources will certainly be applicable to an unusually diverse range of pure and applied scientific problems.

VIII. REFERENCES

1. J. R. Murray, J. Goldhar, and A. Szöke, Appl. Phys. Lett. 32, 551 (1977).
2. R. T. Hawkins, H. Egger, J. Bokor, and C. K. Rhodes, Appl. Phys. Lett. 36, 391 (1980).
3. H. Egger, T. Srinivasan, K. Hohla, H. Scheingraber, C. R. Vidal, H. Pummer, and C. K. Rhodes, Appl. Phys. Lett. 39, 37 (1981).
4. H. Egger, T. S. Luk, K. Boyer, D. F. Muller, H. Pummer, T. Srinivasan, and C. K. Rhodes, Appl. Phys. Lett. 41, 1032 (1982).
5. C. K. Rhodes in Novel Materials and Techniques in Condensed Matter, edited by G. W. Crabtree and P. Vashishta (Elsevier, New York, 1982) p. 151.
6. J. C. Solem and G. C. Baldwin, Science 218, 229 (1982).
7. D. T. Attwood, IEEE J. Quantum Electron. QE-14, 909 (1978).
8. M. H. Key, C. L. S. Lewis, J. G. Lunney, A. Moore, T. A. Hall, and R. G. Evans, Phys. Rev. Lett. 41, 1467 (1978).
9. C. K. Rhodes and R. L. Carman, Appl. Opt. 21, 3799 (1982).
10. R. P. Madden and K. Codling, Astrophys. J. 141, 364 (1965).
11. U. Fano, Phys. Rev. 124, 1866 (1961).
12. R. B. Gold, J. F. Gibbons, T. J. Magee, J. Peng, R. Ormond, V. R. Deline, and C. A. Evans, Jr., in Laser and Electron Beam Processing of Materials, edited by C. W. White and P. S. Peercy (Academic Press, New York, 1980) p. 221.
13. T. S. Luk and T. Srinivasan, private communication.
14. D. J. Kligler, J. Bokor, and C. K. Rhodes, Phys. Rev. A 21, 607 (1980).
15. J. P. Colpa in Physics of High Pressures and Condensed Phases, edited by A. van Itterbeek (North-Holland, Amsterdam, 1965) p. 490; M. Rothschild, W. Gornik, J. Zavelovich, and C. K. Rhodes, J. Chem. Phys. 75, 3794 (1981).
16. J. Eggleston, J. Dallarosa, W. K. Bischel, J. Bokor, and C. K. Rhodes, J. Appl. Phys. 50, 3867 (1979); C. K. Rhodes in High Power Lasers and Applications, edited by K. L. Kompa and H. Walther (Springer-Verlag, Berlin, 1978) p. 163.
17. R. W. Dreyfus and R. T. Hodgson, Phys. Rev. A 9, 2635 (1974).
18. A. L'Huillier, L. A. Lompre, G. Mainfray, and C. Manus, Phys. Rev. Lett. 48, 1814 (1982).
19. G. Wendin, J. Phys. B 4, 1080 (1971); G. Wendin, J. Phys. B 6, 42 (1973).
20. Y. S. Kim and P. Lambropoulos, Phys. Rev. Lett. 49, 1698 (1982).
21. T. S. Luk, H. Pummer, H. Egger, and C. K. Rhodes, private communication.
22. R. D. Cowan, The Theory of Atomic Structure and Spectra (University of California Press, Berkeley, 1981) p. 14.
23. W. Ekardt and D. B. T. Thoai, Physica Scripta 26, 194 (1982).
24. M. G. Mayer, Phys. Rev. 60, 184 (1941).
25. T. B. Lucatorto, T. J. McIlrath, J. Sugar, and S. M. Younger, Phys. Rev. Lett. 47, 1124 (1981).

IX. APPENDICES

APPENDIX A

VACUUM ULTRAVIOLET STIMULATED EMISSION FROM TWO-PHOTON EXCITED MOLECULAR HYDROGEN

H. Pummer, H. Egger, T. S. Luk, T. Srinivasan,
and C. K. Rhodes
Department of Physics
University of Illinois at Chicago
P.O. Box 4348
Chicago, IL 60680

ABSTRACT

Intense vacuum ultraviolet stimulated emission in molecular hydrogen, on both the Lyman and Werner bands, following excitation by two quantum absorption at 193 nm on the $X\ ^1\Sigma_g^+ \rightarrow E,F\ ^1\Sigma_g^+$ transition, has been observed. The shortest wavelength seen in the stimulated spectrum was 117.6 nm corresponding to the $C\ ^1\Pi_u \rightarrow X\ ^1\Sigma_g^+$ (2-5) Q(1) transition. The radiative cascade mechanism found to lead to the vacuum ultraviolet emissions also causes strong infrared stimulated emission to occur on the $E,F\ ^1\Sigma_g^+ \rightarrow B\ ^1\Sigma_u^+$ band. Two entirely separate radiative excitation channels are observed to play important roles in the state selective molecular population of the $E,F\ ^1\Sigma_g^+$ level. One involves two 193-nm quanta in the X→E,F amplitude while the other process combines a 193-nm quantum with a first Stokes shifted photon in H_2. The optical Stark effect was seen to play a significant role in the excitation process with shifts of molecular resonances as large as $\sim 45\ cm^{-1}$. Substantial deviations from Born-Oppenheimer behavior, resulting in a dramatic shift of the stimulated spectrum depending upon the excited state rotational quantum number, were clearly observed for molecular levels close to the potential maximum separating the inner and outer wells of the $E,F\ ^1\Sigma_g^+$ state. The maximum energy observed in the strongest

stimulated line was $\sim$ 100 μJ, a value corresponding to an energy conversion efficiency of $\sim$ 0.5%. The pulse duration of the stimulated emission is estimated from collisional data to be $\sim$ 10 ps, a figure indicating a maximum converted vacuum ultraviolet power of $\sim$ 10 MW.

I. INTRODUCTION

In the infrared spectral region, both parametric processes and direct multiphoton excitation[1] of excited states followed by down- or up-shifted laser emission[2] have been used extensively for generation of coherent radiation in that range. With the development of tunable excimer lasers which can deliver narrow bandwidth[3-5] radiation in short,[6,7] high intensity pulses of superior spatial quality, these techniques have also become attractive for the generation of high power vacuum ultraviolet (VUV) and extreme ultraviolet (XUV) radiation.

Direct radiative excitation by multiquantum processes can be used to generate amplification in the VUV and XUV regions. Molecular hydrogen represents the essential paradigm of this basic mechanism in the VUV range on account of its fundamental nature and the presence of a known[8,9] two-quantum resonance on the $X\ ^1\Sigma_g^+ \rightarrow E,F\ ^1\Sigma_g^+$ transition at 193 nm. In this work, the observation of efficient stimulated emission in the infrared on the $E,F\ ^1\Sigma_g^+ \rightarrow B\ ^1\Sigma_u^+$ band and vacuum ultraviolet on the Lyman and Werner bands[10] following two-photon excitation of the $E,F\ ^1\Sigma_g^+$ state in H_2 using a 193-nm ArF* laser is described.

II. TWO-PHOTON TRANSITIONS IN H_2 AT 193 nm

The relevant potential energy curves in H_2 are illustrated[11] in Fig. 1. At 300 K the relative equilibrium rotational state populations in the ground $X\ ^1\Sigma_g^+$ state for J = 0, 1, 2, and 3 levels are 1.0, 4.9, 0.83, and 0.52, respectively. The lowest excited state, that is optically connected to the ground state by a dipole transition, is the $B\ ^1\Sigma_u^+$ state, which has a radiative lifetime[12] of $\sim$ 600 ps (the exact value depending upon the vibrational quantum number) and a collisional quenching rate[12] $k_B \sim 1.3 \times 10^{-9}$ cm^3/s at 300 K. As shown in Fig. 1, the first excited singlet gerade state $E,F\ ^1\Sigma_g^+$ has a double minimum arising from

the avoided crossing of the $E(1s\sigma 2s\sigma)$ and $F(2s\sigma)^2$ curves.[13] The radiative lifetime from this level has been determined, both experimentally[9] and theoretically,[13,14] to be $\sim$ 90 ns with a corresponding collisional quenching rate that has been measured to be $k_E \sim 2.1 \times 10^{-9}$ cm^3/s.

For the $X\ ^1\Sigma_g^+ \rightarrow E,F\ ^1\Sigma_g^+$ two-photon transition in H_2, the Q-branch [X(J) $\rightarrow$ E,F(J)] transitions are the strongest[15] for linearly polarized radiation. Given the available tuning range of the ArF* system in the vicinity of 193 nm, the transitions in H_2 that can be excited with two 193-nm quanta are the Q(0), Q(1), Q(2), and Q(3) transitions of the $X\ ^1\Sigma_g^+ \rightarrow E,F\ ^1\Sigma_g^+$ (0-2) vibrational band.[15] Of particular interest are the Q(2) and Q(3) transitions which lie[16] at 103,328 cm^{-1} and 103,282 cm^{-1}, respectively, since they occur at frequencies for which interference from oxygen absorption at the corresponding 193-nm wavelengths is absent. Contrarily, Fig. 2 clearly shows that the frequency required for excitation of the Q(1) transition (51739.5 cm^{-1}) lies very close to the molecular Schumann-Runge[17,18] R(19) line of the (4-0) band at 51740 cm^{-1}. Similar interference from oxygen absorption also occurs for the 193-nm wavelength corresponding to the Q(0) transition. Although these coincidences with oxygen lines appear to prevent the two-quantum excitation of the H_2 Q(0) and Q(1) transitions without the use of an oxygen-free path for the laser beam, the occurrence of the optical Stark effect, as discussed quantitatively below in Section IV.A, obviates this limitation.

The two-photon coupling parameter, corresponding to the pump laser bandwidth of 5 cm^{-1} and a Doppler broadened H_2 linewidth has been estimated[8,9,19,20] to be $\alpha = 2 \times 10^{-31}$ cm^4/W. An important aspect to be noted from Fig. 1 is the near degeneracy between the $C\ ^1\Pi_u^+$ state and the inner minimum of $E,F\ ^1\Sigma_g^+$ state. Since the $E(2s\sigma)$ and $C(2p\pi)$ states strongly resemble their atomic counterparts[13,21] at the relevant internuclear separation of $\sim$ 1 $\mathring{A}$, the two electronic states are

connected by a large transition moment[22] with a magnitude of $\sim$ 5 au. This causes the C $^1\Pi_u^+$ state to be the dominant intermediate state in the two-photon amplitude for excitation of the E,F $^1\Sigma_g^+$ from the X $^1\Sigma_g^+$ level, a conclusion first stated by Huo and Jaffe.[20]

As described below, a two-quantum coupling parameter of this magnitude and irradiation with 10-ps pulses enables approximately one percent of the H_2 ground state population to be transferred to a rotationally specific excited state at an intensity of $\sim 10^{11}$ W/cm^2 when proper account is made for losses due to photoionization of the E,F $^1\Sigma_g^+$ level at 193 nm. Therefore, at a medium density of 2×10^{19} cm^{-3}, with an allowance for rotational partition, inversion densities on the scale of $\sim 10^{17}$ cm^{-3} can be generated. Since the optical cross sections for the inverted transitions are $\sim 10^{-14}$ cm^2, a value leading to an optical gain constant of $\sim 10^3$ cm^{-1}, strong stimulated emission is expected under these circumstances. Indeed, recent estimates by Huo and Jaffe[20] indicate that the coupling parameter a could be significantly larger than the earlier estimates leading to the value used above, a correction that would increase the gain constant by an appreciable factor.

It is known that molecular hydrogen is an efficient medium for stimulated Raman scattering of ultraviolet radiation.[23,24] Measurements with 10-ns ArF* laser pulses indicate that intense stimulated Raman scattering occurs in our apparatus at H_2 pressures $\gtrsim$ 600 Torr and that $\sim$ 25% of the 193-nm fundamental wave is converted into the first order Stokes line S_1 when the 193-nm beam is focussed (f/100) into a cell containing $\sim$ 1000 Torr of H_2. Therefore, in the high pressure regime (> 600 Torr), two-quantum processes involving a Stokes shifted quantum could have an appreciable rate. Indeed, since the vibrational spacing[25] of the H_2 ground X $^1\Sigma_g^+$ state is almost exactly twice that characteristic of the excited E,F $^1\Sigma_g^+$ level, a two-quantum resonance occurs for the fundamental

of 51656 cm^{-1} with the corresponding Stokes S_1 at 47501 cm^{-1} for the transition from $X\ ^1\Sigma_g^+$ (v = 0, J = 0) to $E,F\ ^1\Sigma_g^+$ (v = 0, J = 0). It will be seen that this Raman assisted channel is an important mode of molecular excitation.

III. EXPERIMENTAL APPARATUS

The 193-nm ArF* source[7] used in these experiments furnished an effective power of $\sim$ 2 GW in a pulse duration of $\sim$ 10 ps. This radiation had a measured bandwidth of $\sim$ 5 cm^{-1} and a divergence of $\sim$ 10 μrad, values close to their respective transform limits. The beam was focussed with an f = 1.6 m lens into the center of the experimental cell. The experimental cell consisted of a 2 m long cell containing the hydrogen up to densities of $\sim$ 2 amagat and was equipped with entrance and exit windows of CaF_2 and LiF, respectively. The pressure of H_2 inside the cell was determined by a standard baratron gauge. For observation of the VUV radiation, the LiF exit window of the cell was attached directly to the entrance slit of a 1 m VUV monochromator (McPherson 225) equipped with an optical multichannel analyzer (OMA PAR) at the exit slit to serve as the detector. The detection of infrared radiation with $\lambda \geq 7000$ Å was accomplished similarly with the use of a suitable grating and a glass window at the entrance slit to eliminate all ultraviolet radiation.

IV. EXPERIMENTAL RESULTS

A. $B\ ^1\Sigma_u^+ \rightarrow X\ ^1\Sigma_g^+$ emissions

Excitation of the hydrogen gas at frequencies corresponding to the two-quantum transitions discussed above leads to the observation of intense stimulated emission with a characteristic line structure. Tables Ia and Ib contain the

identification[16] of the infrared and VUV transitions observed in the low pressure regime, 20-500 Torr, along with information on the observed intensities. The experimentally observed wavelengths agree with the previously determined values,[10,16] within our experimental accuracy of $\sim$ 20 cm^{-1}. This fact, concerning the wavelengths, will be considered further below in the discussion of the optical Stark effect.

With the ArF* laser tuned to the Q(3) transition, stimulated emission on the lines shown in Fig. 3 was observed. The emission pattern displays the additional transitions illustrated in Fig. 4 for excitation corresponding to the Q(2) transition. Two observations concerning the nature of these stimulated spectra are noteworthy. The first involves the shift of the dominant E,F→B transition in the infrared from (2→2) P(4) to (2→1) P(3) upon changing from Q(3) to Q(2) excitation, an indication of a significant dependence of the wavefunction for nuclear coordinates on the rotational quantum number. The second point relates to the occurrence of stimulated emission stemming from the J = 3 level (Fig. 3) with the 193-nm laser tuned to the frequency corresponding to the Q(2) transition (Fig. 4). It is significant that the corresponding dual output did <u>not</u> occur under the excitation of the Q(3) transition. No lines originating from J = 2 state due to the excitation of the Q(2) transition have been observed with the laser tuned to the Q(3) transition.

Qualitatively, the shift in the dominant infrared transition accompanying the change from Q(3) to Q(2) excitation can be explained by the fact that the inner-well E $^1\Sigma_g^+$ (v = 2, J = 3) level is only a few hundred wavenumbers ($\sim$ 200 ± 150 cm^{-1}) below the intermediate maximum of the E,F potential curve,[11] whereas the nearby J = 2 level is lower by an additional 305 cm^{-1}. It has been established[26] theoretically that strong deviations from Born-Oppenheimer behavior

occur for the E,F $^1\Sigma_g^+$ state, particularly in the region close to the maximum of the potential barrier and specific manifestations of this deviation have been recently observed by Marinero et al.[27] Therefore, due to the vibronic coupling between the inner and outer wells of this state and the consequently large deviation from Born-Oppenheimer behavior for the (v = 2, J = 3) level of the E,F state, the (2-2) vibronic transition is preferred over the (2-1) transition predicted by Lin.[28] The peculiar nature of the J = 3 level arising from its proximity to the potential maximum is also reflected in the anomalous spacings of the rotational levels. The energy difference between the J = 2 and J = 3 levels is 305 cm^{-1}, a value that stands in contrast compared to the 85 cm^{-1} difference separating the J = 1 and J = 2 states.[16]

The observation of stimulated emission originating from the E,F $^1\Sigma_g^+$ (v = 2, J = 3) level upon excitation of the system at a frequency corresponding to the two-quantum Q(2) transition, is direct evidence of the role of the optical Stark effect. Fig. 5 illustrates the positions of the participating levels both in the presence and the absence of the 193-nm radiation field based upon previously performed estimates of the nonlinear coupling to this molecule.[29] As shown in Fig. 5, at an intensity of $\sim 6 \times 10^{11}$ W/cm^2, the unshifted Q(2) transition frequency becomes almost exactly equal to the radiatively shifted Q(3) transition frequency. This condition can arise since the optical Stark effect is sufficient to <u>increase</u> the transition energy of the Q(3) line by $\sim$ 45 cm^{-1}, a value large in comparison to both the effective linewidth of the 193-nm radiation and the instrumental resolution used to register the stimulated transitions. Since strong two-photon excitation occurs in regions of the converging 193-nm beam in which the intensity spans the range of 10^{11} W/cm^2 to 10^{13} W/cm^2, the simultaneous excitation of the Q(2) and Q(3) transitions becomes possible, albeit in different

spatial regions, and subsequent stimulated emission on both bands can arise. It is recalled that similar effects have been previously observed[30] for a two-photon-excited 16-μm laser in NH_3. It is important to note that, because of the sign of the radiative shift, the simultaneous excitation of the Q(2) and Q(3) transitions is not expected when the 193-nm laser wavelength is tuned to the Q(3) line, a conclusion which is in agreement with experimental observations. Finally, we observe that optical Stark shifts on the scale observed ($\sim$ 45 cm^{-1}) are sufficient to shift the Q(0) and Q(1) transitions to frequencies for which no interfering oxygen absorption occurs (see Fig. 2), enabling those states to be excited as well.

At H_2 pressures above 600 Torr, an additional set of lines appears when the 193-nm excitation laser is tuned to the E,F←X (2-0) Q(2) transition. These additional observed transitions are shown in Fig. 6 and Table II lists the pertinent data and identifications based on previous studies.[16] Inspection shows that the E,F←X (0-0) Q(0) transition is only 16 cm^{-1} below the energy of one 193-nm fundamental plus one Stokes shifted ArF* photon. As in the case discussed above, this transition energy is increased by 16 cm^{-1} by the optical Stark effect at an intensity of $\sim 2 \times 10^{11}$ W/cm^2. As expected, no emission from the E,F (v = 0) level is observed when the frequency of the 193-nm radiation is decreased by 22.5 cm^{-1} to the E,F←X (2-0) Q(3) transition. Furthermore, the onset of these emissions agrees with the observed threshold for the production of stimulated first Stokes radiation in H_2, an experimental finding strongly reinforcing the conclusion concerning the role of the Raman shifted radiation.

B. $C\ ^1\Pi_u \rightarrow X\ ^1\Sigma_g^+$ emissions

Two strong stimulated lines at 117.7 nm and 117.6 nm originating from the $C\ ^1\Pi_u$ state are observed. These transitions are identified as the Q(2) and

Q(1) (2-5) Werner band lines, respectively, as shown in Fig. 3 and Fig. 4. Based on the fact that C→X stimulated emission is seen over the same wide pressure range (20 Torr to 1000 Torr) as the E,F→B→X cascade, combined with knowledge of the collisional quenching rate governing the E,F state,[8,9] rapid population of the C state by a collisional mechanism must, at least in the lower pressure range, be excluded. Therefore, this leads to the conclusion that the rapid transfer of population from the E,F to the C state can only be explained by a rapid radiative mechanism, namely, stimulated emission on the R(2) line at 38.7 μm and the R(1) line at 161 μm. We recall that the electronic matrix element governing the far infrared E,F→C transitions is extremely large with the basic scale of the coupling strength being the same as the 2s-2p dipole amplitude in the hydrogen atom,[22] ∿ 5 au. The Franck-Condon factors will be close to unity, since the E,F and C potentials coincide almost exactly in the region of the inner minimum. Thus, the large amplitude for the far infrared radiative transition leads to strong amplification and a cascade mechanism populating the C $^1\Pi_u$ state fully analogous to that populating the B $^1\Sigma_u^+$ level through infrared emission on the E,F→B transition. Direct observation, however, of the 38.7 μm and 161 μm emissions was not made, since the wavelengths were too long to be observed in the present equipment.

C. General properties of the stimulated transitions

All the lines in the infrared and vacuum ultraviolet classified as stimulated exhibited clear thresholds for emission and a spatial divergence matching that of the focussed 193-nm excitation beam. Furthermore, since the stimulated transitions observed did <u>not</u> exhibit detectable optical Stark shifts with an instrumental resolution of ∿ 15 cm^{-1}, although radiative shifts on the scale

of $\sim$ 45 cm^{-1} were observed in the process of two-quantum excitation, the experiments indicate that the time of the stimulated emission does not exactly coincide with that of the maximum intensity of 193-nm irradiation. Presumably, the stimulated output occurs at a time slightly later than that of peak excitation, since it is expected that the peak gain, proportional to the quotient of the population inversion and the linewidth, would be maximal at a point shortly after the peak excitation. Physically, the linewidth factor will provide the principal contribution, since appreciable broadening arising from the rate of photoionization will substantially reduce the gain for the range of intensities present at the peak of the 193-nm irradiation. Specifically, at an intensity of $\sim 10^{11}$ W/cm^2, the gain is depressed an order of magnitude by broadening from excited state photoionization.[29]

Previous collisional studies[8,9,12] of the E,F $^1\Sigma_g^+$ and B $^1\Sigma_u^+$ states establish a lifetime of $\sim$ 16 ps at a density of one amagat, a value indicating that the pulse width of the stimulated emission, at least in the higher pressure range examined in these studies, is not appreciably greater than that time. Therefore, the combination of the radiative and collisional influences leads to an expected pulse length of $\sim$ 10 ps for the stimulated output or, as discussed below, an output power of $\sim$ 10 MW on the strongest VUV line. In this picture, since the transit time of the 193 nm excitation pulse through the physically active region is significantly greater than the 10-ps pulse width or the collisional lifetime at typical operating pressures, the radiating medium responds essentially as a travelling wave amplifier.

D. Efficiency of observed stimulated emission

A principal finding of these experimental studies is the observation of a conversion efficiency of 193-nm radiation to specific deep VUV lines approaching

one percent. Since photoionization[9,19,31] and collisional losses[8,9] compete with the two-quantum mechanism for excitation, there exist fundamental relationships connecting the medium density, the VUV gain, the pulse width of the 193-nm excitation, and the conversion efficiency. We now estimate an upper bound for the efficiency expected under conditions comparable to those occurring in these studies.

For this estimate the overall conversion efficiency can be represented as a product of two factors. One factor describes the efficiency with which the incident 193-nm radiation is absorbed in the process of populating the upper level. The second factor takes into account the reduction in upper state population due to photoionization and collisions. For a two-photon coupling parameter $\alpha = 2 \times 10^{-31}$ cm^4/W, based on the previously determined[9] values, the absorption efficiency is estimated to be $\sim$ 25%. In the above estimate, a 193-nm intensity of 5×10^{10} W/cm^2, an equilibrium population density of a ground state rotational level $\sim 3 \times 10^{18}$ cm^{-3}, and an active medium of length 10 cm have been assumed. Under these conditions, the fractional loss of E,F state population due to photoionization and collisional quenching can be calculated to be 80% for a photoionization cross section[9] of 2×10^{-18} cm^2 and a collisional rate constant[9] of 2.1×10^{-9} cm^3/s with an ultraviolet pulse duration of 10^{-11} s and a total medium density of 3×10^{19} cm^{-3}. Since a single stimulated line is generally much stronger than the others in our experiment (see Table Ia and Table Ib), it will be assumed that the stimulated emission occurs on only one transition. Therefore, combining the absorption efficiency and radiation efficiency with the assumption that half of the inversion density can be extracted at $\lambda \sim 800$ nm under conditions of saturation, the resulting energy conversion efficiency for the infrared E→B transition is estimated to be 1.3%. Although the emitted quantum is significantly greater for the B→X transitions ($\lambda \sim 150$ nm), similar estimates for the B→X VUV

band also indicate an energy conversion efficiency of ∿ 0.5%. In this latter case, additional losses arise from photoionization of the B $^1\Sigma_u^+$ state with a cross section that will be somewhat larger than that corresponding to the E,F $^1\Sigma_g^+$ level.[32] It should be noted, however, that the recent estimates of the two-photon X↦E,F cross section performed by Huo and Jaffe[20] indicate a cross section larger by a factor of six than the one used in the appraisal of the efficiency made above. This suggests, that under optimum conditions, a maximum efficiency of ∿ 3% could be achieved on the B↦X band. In the present experiment, which does not correspond to the optimum conditions for efficient excitation, comparison with attenuated 193 nm radiation shows that the strongest transition B (v = 1, J = 3) → X (v = 7, J = 4) (Table Ib) at λ ∿ 150 nm contains an energy of ∿ 100 μJ corresponding to an observed energy conversion efficiency of ∿ 0.5%.

V. CONCLUSIONS

Intense stimulated emission on the Werner and Lyman bands of H_2 is observed following two-photon excitation of the X↦E,F transition at 193 nm with ∿ 10 ps radiation. Stimulated emission on infrared transitions belonging to the E,F↦B band is also observed. All the stimulated lines seen can be attributed to direct radiative cascades originating from the state initially populated in the two-quantum excitation. Two different channels of excitation were found to populate the E,F $^1\Sigma_g^+$ levels, one involving two 193-nm quanta and the other conbining a 193-nm quantum with a first Stokes shifted photon. The optical Stark effect was seen to play a significant role in the excitation process with shifts of molecular resonances as large as ∿ 45 cm^{-1}. In addition, a large deviation from Born-Oppenheimer behavior, resulting in an abrupt shift of the stimulated spectrum depending upon the excited state rotational quantum

number, was observed for molecular levels close to the potential maximum separating the inner and outer wells of the E,F $^1\Sigma_g^+$ state. The energy observed on the strongest line was $\sim$ 100 μJ, a value corresponding to a conversion efficiency of $\sim$ 0.5%. The corresponding pulse duration has been estimated to be $\sim$ 10 ps, a figure indicating a maximum converted VUV power of $\sim$ 10 MW. Clearly, the general technique of nonlinear excitation studied in this work can be readily extended to a wide range of transitions in H_2, HD, and D_2 to provide a multitude of intense narrow bandwidth sources in the vacuum ultraviolet region.

VI. ACKNOWLEDGEMENTS

The authors wish to acknowledge the expert technical assistance of M. J. Scaggs and J. R. Wright. We are grateful to K. Yoshino, O. E. Freeman, J. R. Esmond, and W. H. Parkinson and to Pergamon Press for making available and granting permission to reprint Figure 2. This work was supported by the Office of Naval Research; the Air Force Office of Scientific Research under grant no. AFOSR-79-0130; the National Science Foundation under grant no. PHY81-16626; and the Avionics Laboratory, Air Force Wright Aeronautical Laboratories, Wright Patterson Air Force Base, Ohio.

References

1. "Nonlinear Infrared Generation", Y.-R. Shen, ed., Topics in Applied Physics (Springer-Verlag, New York, 1977).
2. H. Pummer, W. K. Bischel, and C. K. Rhodes, J. Appl. Phys. 49, 976 (1978); D. Prosnitz, R. R. Jacobs, W. K. Bischel, and C. K. Rhodes, Appl. Phys. Lett. 32, 221 (1978); J. Eggleston, J. Callarosa, W. K. Bischel, J. Bokor, and C. K. Rhodes, J. Appl. Phys. 50, 3867 (1979).
3. R. T. Hawkins, H. Egger, J. Bokor, and C. K. Rhodes, Appl. Phys. Lett. 36, 391 (1980).
4. J. C. White, J. Bokor, R. R. Freeman, and D. Henderson, Opt. Lett. 6, 293 (1981).
5. H. Egger, T. Srinivasan, K. Hohla, H. Scheingraber, C. R. Vidal, H. Pummer, and C. K. Rhodes, Appl. Phys. Lett. 39, 37 (1981).
6. P. H. Bucksbaum, J. Bokor, R. H. Storz, and J. C. White, Opt. Lett. 7, 399 (1982).
7. H. Egger, T. S. Luk, K. Boyer, D. F. Muller, H. Pummer, T. Srinivasan, and C. K. Rhodes, Appl. Phys. Lett. 41, 1032 (1982).
8. D. J. Kligler and C. K. Rhodes, Phys. Rev. Lett. 40, 309 (1978).
9. D. J. Kligler, J. Bokor, and C. K. Rhodes, Phys. Rev. A21, 607 (1980).
10. R. W. Dreyfus and R. T. Hodgson, Phys. Rev. A9, 2635 (1978); R. T. Hodgson and R. W. Dreyfus, Phys. Rev. Lett. 28, 536 (1972); H. Pummer, H. Egger, T. S. Luk, T. Srinivasan, and C. K. Rhodes, "High-Power VUV Stimulated Emission from Two-Photon Excited H_2", Proceedings of the Topical Meeting on Excimer Lasers, Lake Tahoe, Nevada, January 10-12, 1983, edited by H. Egger, H. Pummer, and C. K. Rhodes (American Institute of Physics, New York), to be published; T. Srinivasan, "Generation of Coherent Vacuum

Ultraviolet and Extreme Ultraviolet Radiation", thesis, Department of Physics, University of Illinois at Chicago, unpublished.

11. T. E. Sharp, Atomic Data 2, 119 (1971).

12. H. Schmoranzer and J. Imschweiler, Proceedings of the Eighth International Conference on Atomic Physics, Göteborg, August 2-6, 1982, Program and Abstracts, edited by I. Lindgren, A. Rosén, and S. Svanberg (Wallin & Dalholm Boktr. AB, Lund, 1982) p. A40.

13. W. Kołos and L. Wolniewicz, J. Chem. Phys. 50, 3328 (1969).

14. R. J. Spindler, J. Quant. Spectrosc. Radiat. Transfer 9, 1041 (1969).

15. G. Herzberg, Spectra of Diatomic Molecules (Van Nostrand Reinhold Co., New York, 1950).

16. G. H. Dieke, J. Mol. Spectrosc. 2, 494 (1958).

17. M. Ackerman and F. Biaumé, J. Mol. Spectrosc. 35, 73 (1970).

18. K. Yoshino, D. E. Freeman, J. R. Esmond, and W. H. Parkinson, Planetary and Space Science, in press.

19. W. K. Bischel, J. Bokor, D. J. Kligler, and C. K. Rhodes, IEEE J. Quantum Electron. QE-15, 380 (1979).

20. W. M. Huo and R. L. Jaffe, private communications.

21. W. Kołos and L. Wolniewicz, J. Chem. Phys. 43, 2429 (1965).

22. H. A. Bethe and E. E. Salpeter, Quantum Mechanics of One- and Two-Electron Atoms (Plenum, New York, 1977).

23. T. R. Loree, R. C. Sze, and D. L. Baker, Appl. Phys. Lett. 31, 37 (1977).

24. R. S. Hargrove and J. A. Paisner, Topical Meeting on Excimer Lasers, Charleston, SC, Sept. 11-13, 1979 (Optical Society of America, Washington, DC, 1979) p. ThA-6.

25. K. P. Huber and G. Herzberg, Molecular Spectra and Molecular Structure, IV. Constant of Diatomic Molecules (Van Nostrand Reinhold Co., New York, 1979).

26. L. Wolniewicz and K. Dressler, J. Mol. Spectrosc. 67, 416 (1977).

27. E. E. Marinero, C. T. Rettner, and R. N. Zare, private communication.

28. C. S. Lin, J. Chem. Phys. 60, 4660 (1974).

29. T. Srinivasan, H. Egger, H. Pummer, and C. K. Rhodes, "Generation of Extreme Ultraviolet Radiation at 79 nm by Sum Frequency Mixing", submitted to IEEE J. Quantum Electron.; P. Avon, C. Cohen-Tannoudji, J. Dupont-Roc, and C. Fabre, J. de Phys. 9, 993 (1976).

30. H. Pummer, W. K. Bischel, and C. K. Rhodes, J. Appl. Phys. 49, 976 (1978); J. Bokor, W. K. Bischel, and C. K. Rhodes, J. Appl. Phys. 50, 4541 (1979).

31. J. Bokor, J. Zavelovich, and C. K. Rhodes, Phys. Rev. A21, 1453 (1980).

32. A. Cohn, J. Chem. Phys. 57, 2456 (1972).

TABLE 1a. Transitions, corresponding wavelengths and relative intensities of the observed stimulated emission in low pressure (∿ 20 Torr) H_2 on pumping the Q(3) transition of the $X\ ^1\Sigma_g^+ \rightarrow E,F\ ^1\Sigma_g^+$ (0-2) band. Values in column 3 are taken from the work of Dieke [Ref. (16)].

Transition	Wavelength Å		Observed relative strength
	Present work	Previous work	
Infrared			
E → B			
2-2 P(4)	9222	9222.04	5
VUV			
B → X			
2-8 P(5)	1531.5	1532.1	1
2-9 R(3)	1570.8	1571.4	5
2-9 P(5)	1584.9	1585.5	12

TABLE Ib. Transitions, corresponding wavelengths and the relative intensities of the observed stimulated emission in low pressure (20 Torr) H_2 on pumping the Q(2) transition of the X $^1\Sigma_g^+$ - E,F $^1\Sigma_g^+$ (0-2) band. Values in column 3 are taken from the work of Dieke [Ref. (16)].

Transition	Wavelength Å		Observed relative strength
	Present work	Previous work	
Infrared			
E → B			
2-1 P(3)	8370	8369.23	8
2-0 P(3)	7544.1	7544.06	0.8
VUV			
B → X			
1-6 P(4)	1440.9	1440.7	3
1-6 R(2)	1428.8	1428.9	<1
1-7 P(4)	1499.6	1499.6	33
1-7 R(2)	1487.6	1487.7	13
1-8 P(4)	1557.4	1557.6	6
1-8 R(2)	1545.4	1545.7	1
VUV			
C → X			
2-5 Q(2)	1177.9	11[illegible]8	<1
2-5 Q(1)	1176.6	1175.8	<1

TABLE II. Transitions, corresponding wavelengths and relative intensities of the observed stimulated emission in high pressure (> 600 Torr) H_2. Values in column 3 are taken from the work of Dieke [Ref. (16)].

Transition	Wavelength Å		Observed relative strength
	Present work	Previous work	
E → B			
0-0 P(1)	11210	11159.1	
B → X			
0-3 R(0)	1275.2	1274.6	<1
0-3 P(2)	1280	1279.5	<1
0-4 R(0)	1333.6	1333.5	6
0-4 P(2)	1339	1338.6	3
0-5 R(0)	1394.4	1393.7	21
0-5 P(2)	1399.8	1399	11
0-6 R(0)	1455.5	1454.9	2.5
0-6 P(2)	1460.9	1460.2	1

Figure Legends

FIG. 1. Partial representation of potential energy curves of H_2 (taken from Sharp, ref. 11).

FIG. 2. Absorption cross section of O_2 in the range 51300-52000 cm^{-1}. The solid arrows indicate the transition frequencies of the Q-branch of the $X\ ^1\Sigma_g^+$ (v = 0) $-$ E,F $^1\Sigma_g^+$ (v = 2) band. The broken arrows indicate the tuning range of the ArF* laser. Reprinted with permission from Pergamon Press (ref. 18).

FIG. 3. Stimulated emission from H_2 following E,F←X (2-0) Q(3) two-photon excitation with 2 ArF* (193 nm) quanta. For the E,F→C transition (broken line), see text.

FIG. 4. Stimulated emission from H_2 following E,F←X (2-0) Q(2) two-photon excitation with 2 ArF* (193 nm) quanta. For the E,F→C transition (broken line), see text.

FIG. 5. Transition frequencies of Q(2) and Q(3) lines of $X\ ^1\Sigma_g^+$ (v = 0) → E,F $^1\Sigma_g^+$ (v = 2) transition (a) in the absence and (b) in the presence of strong optical field (shifts given for $I = 6 \times 10^{11}$ W/cm^2).

FIG. 6. Stimulated emission from H_2 following E,F←X (0-0) Q(0) two-photon excitation with a fundamental and one Stokes shifted ArF* photon.

Figure 1

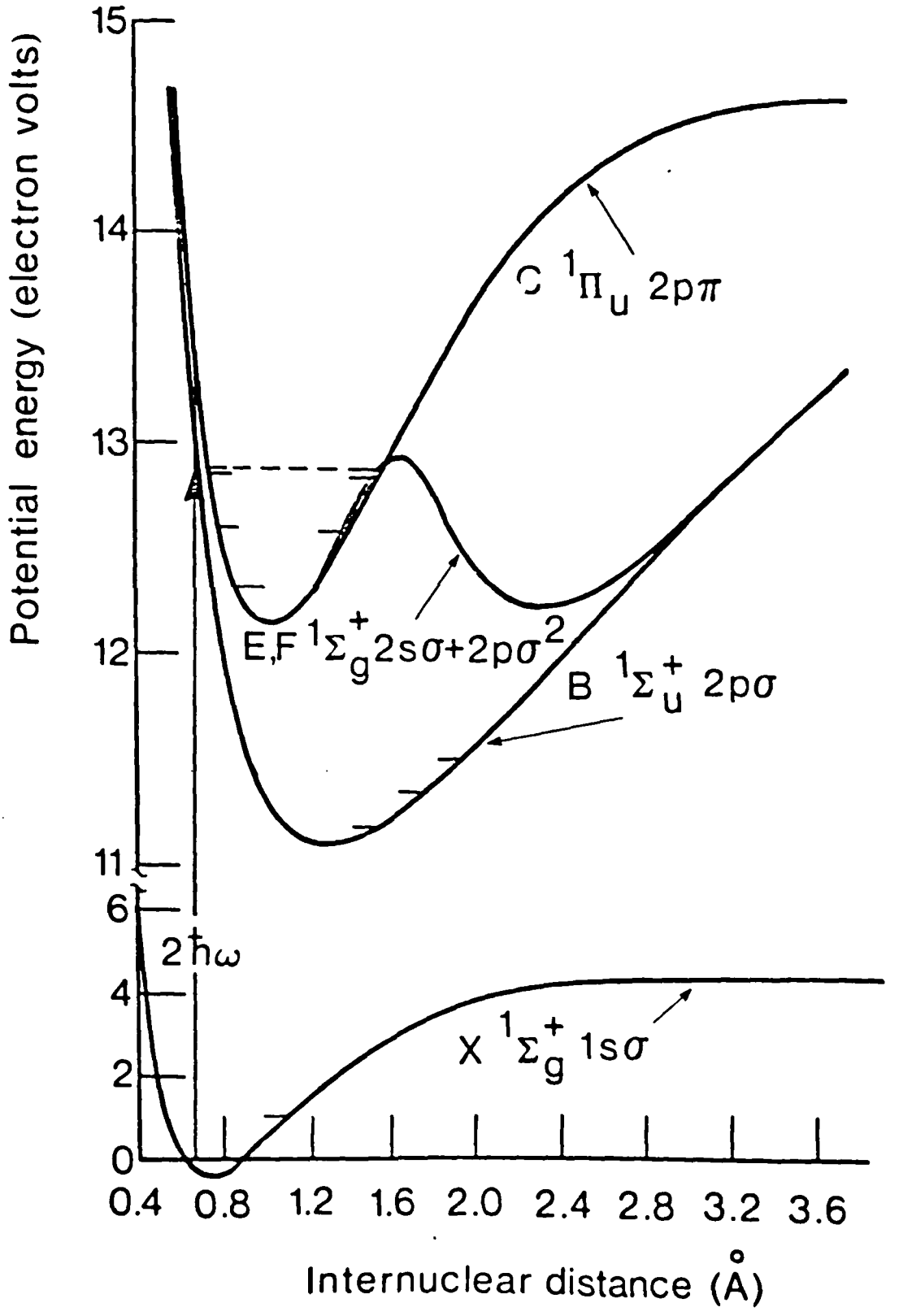
Potential energy (electron volts)
15
14
13
12
11
6
4
2
0
C $^1\Pi_u$ 2pπ
E,F $^1\Sigma_g^+$ 2sσ+2pσ^2
B $^1\Sigma_u^+$ 2pσ
X $^1\Sigma_g^+$ 1sσ
2ħω
0.4
0.8
1.2
1.6
2.0
2.4
2.8
3.2
3.6
Internuclear distance (Å)

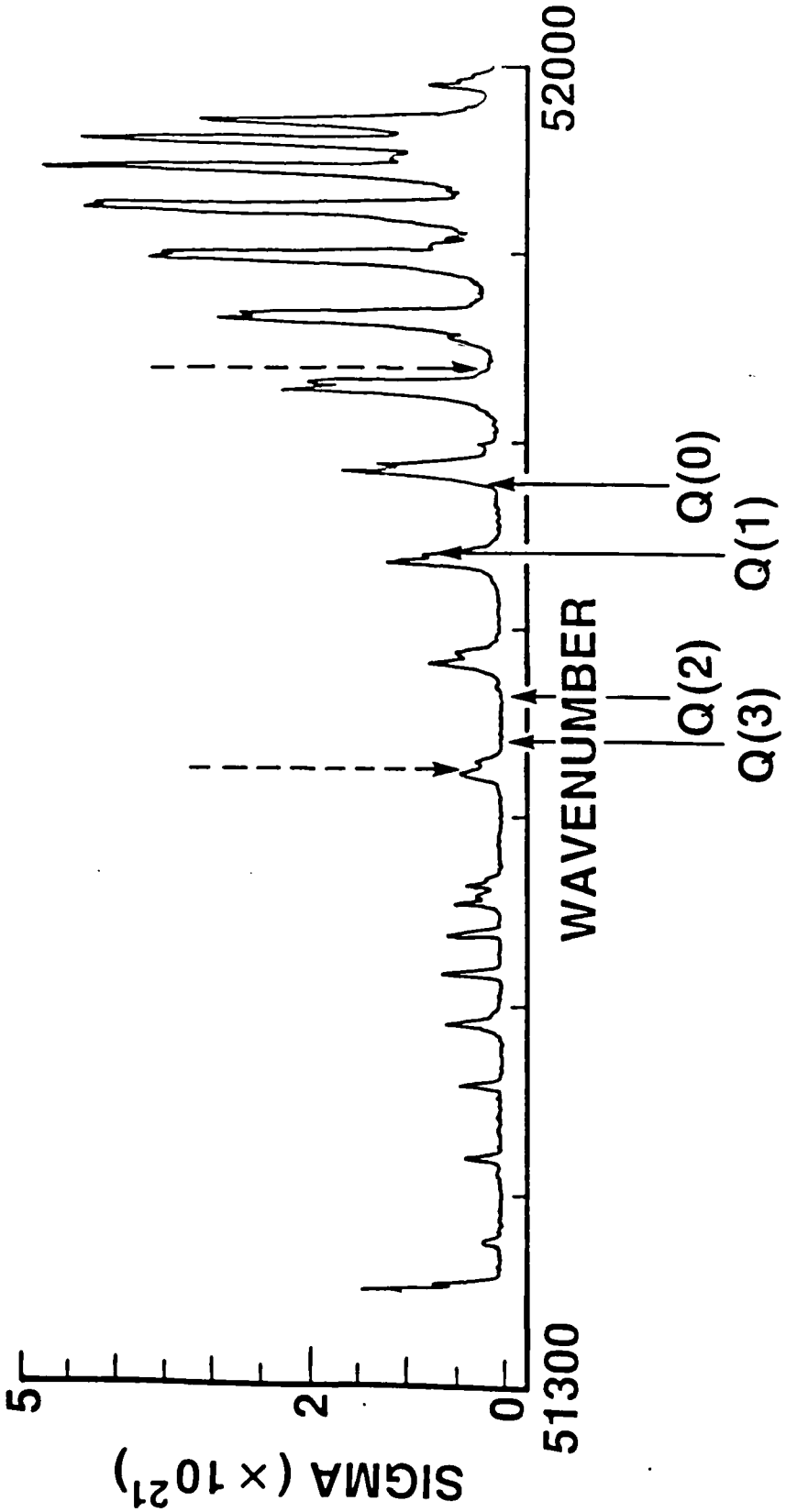

Figure 2

Figure 3

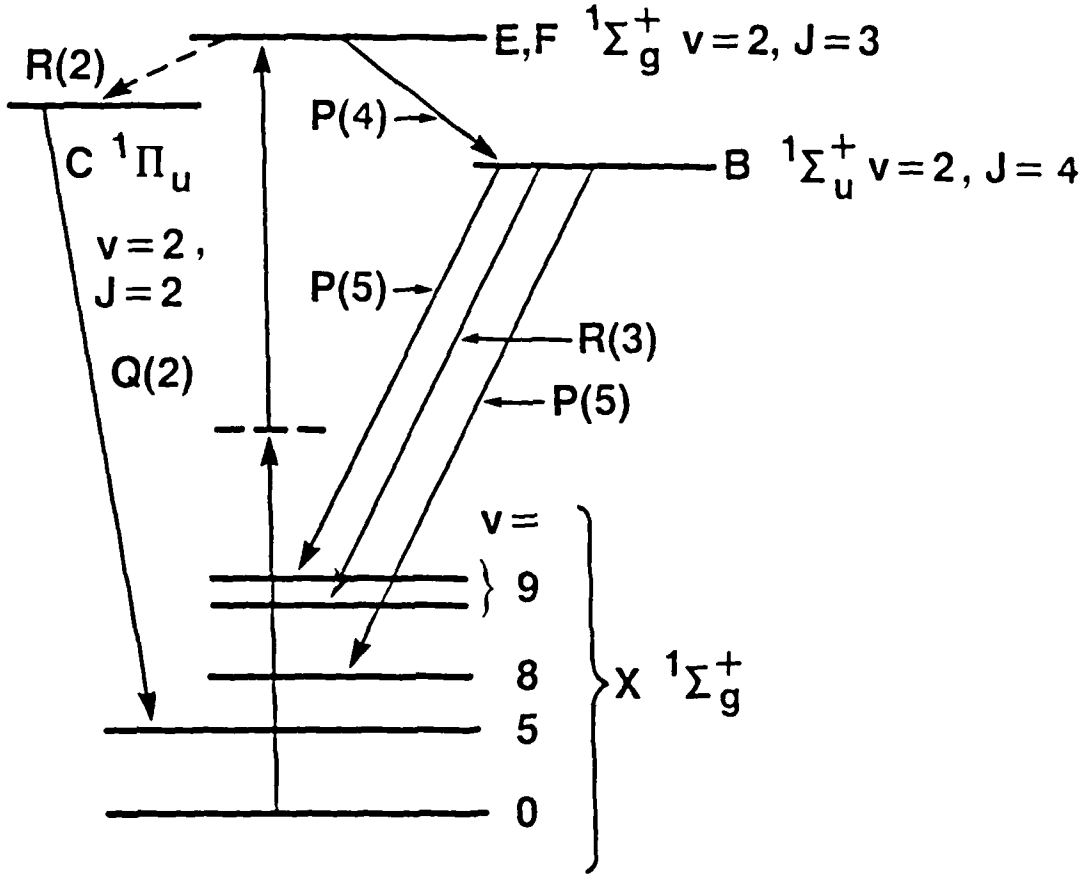

Wavelengths in nm:

E,F → B	B → X			C → X
2-2 P (4)	2-8 P(5)	2-9 P (5)	2l-9 R (3)	2-5 Q (2)
922.2	153.2	158.5	157.1	117.7

Figure 4

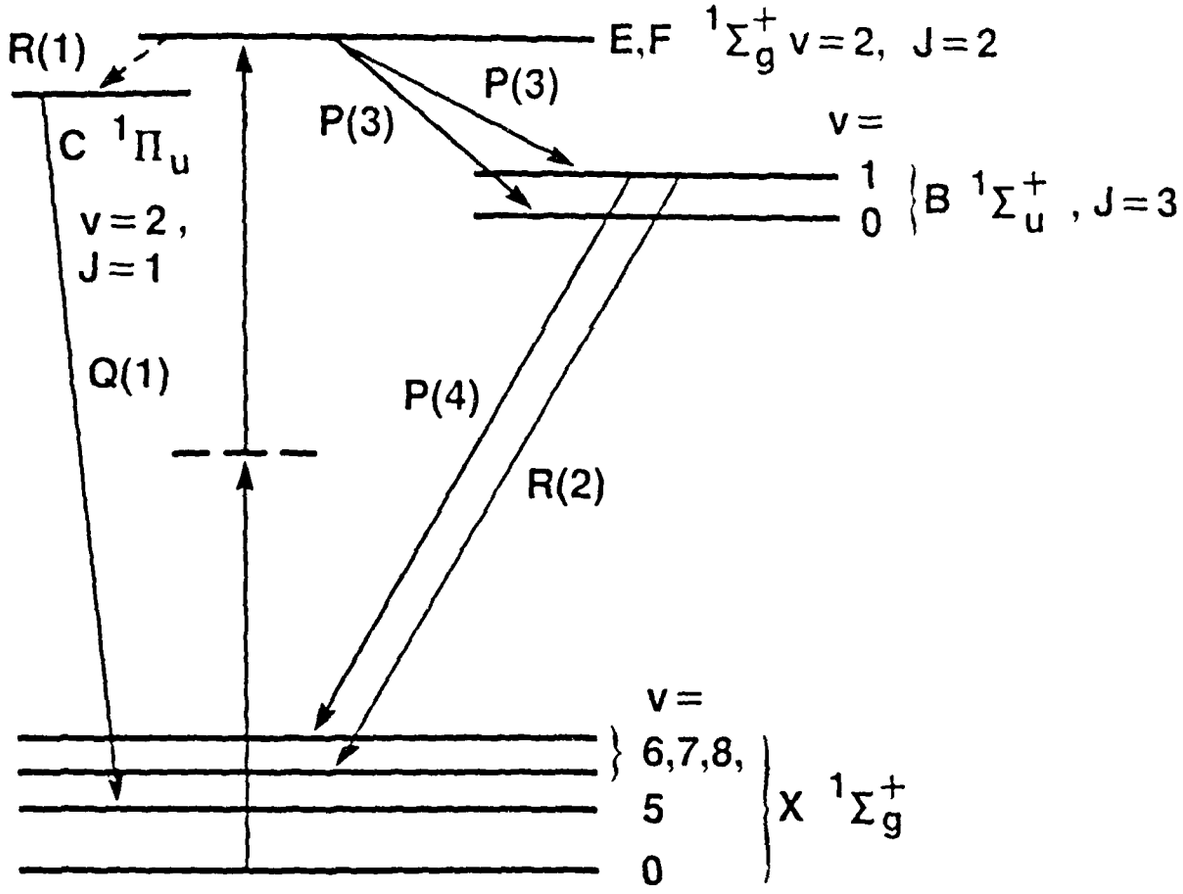

Wavelengths in nm:

E,F → B		C → X
2-1 P (3)	2-0 P (3)	2-5 Q (1)
836.9	754.4	117.6

B → X	1 - 6	1 - 7	1 - 8
P (4)	144.1	150.0	155.8
R (2)	142.9	148.8	154.6

Figure 5

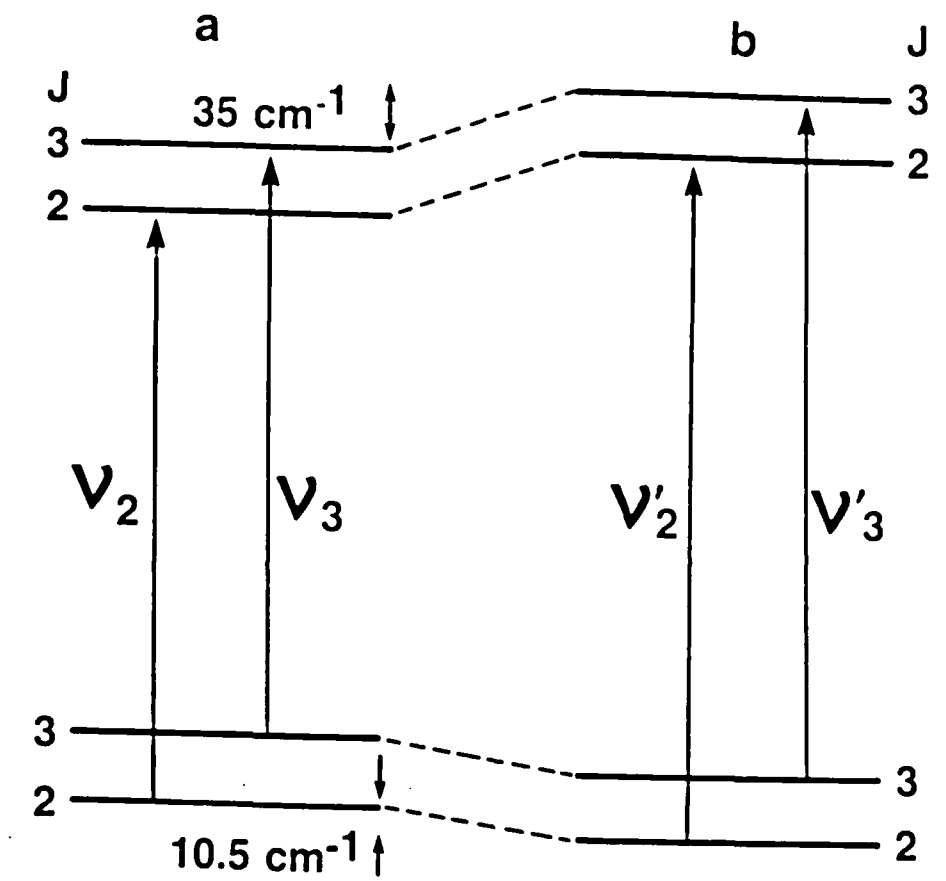
a
b
J
J
3
2
35 cm-1
3
2
ν2
ν3
ν'2
ν'3
3
2
3
2
10.5 cm-1
ν2 = 103327.8 cm-1
ν3 = 103281.8 cm-1
ν'2 = 103373.3 cm-1
ν'3 = 103326.3 cm-1

Figure 6

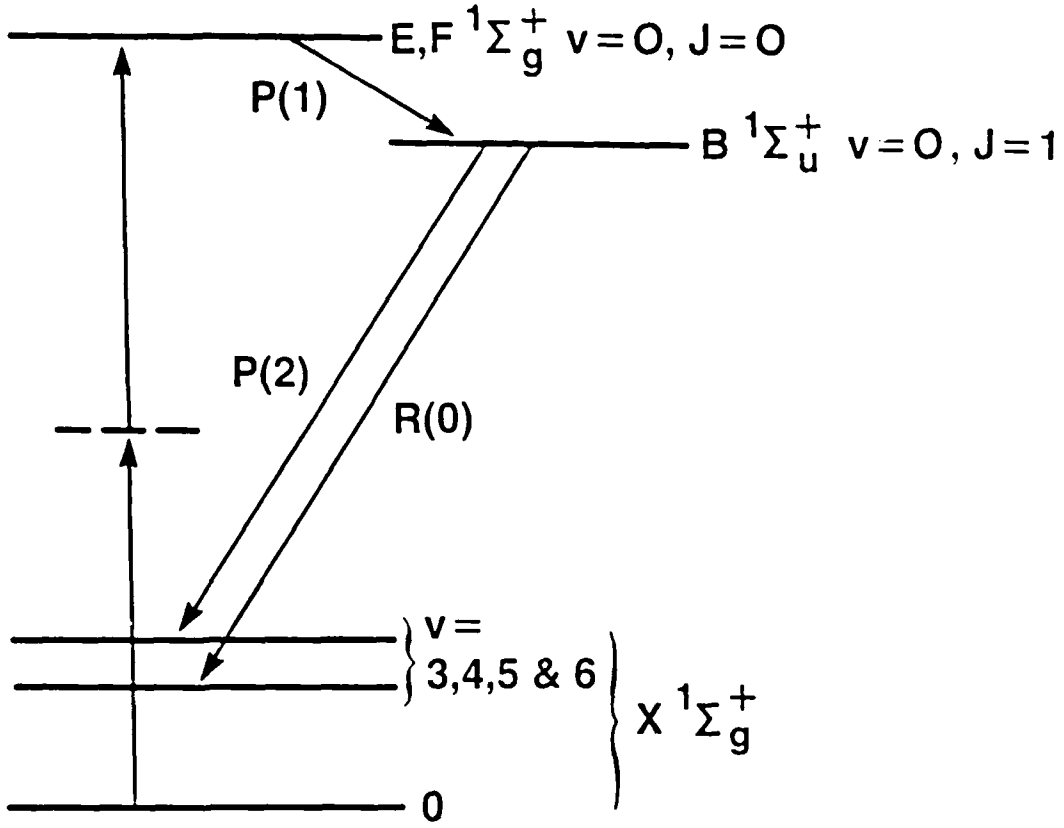

Wavelengths in nm:

B→X	0 - 3	0 - 4	0 - 5	0 - 6
P(2)	127.9	133.9	139.9	146.0
R(0)	127.5	133.3	139.4	145.5

E,F→B (0 - 0) P(1): 1121 nm

APPENDIX B

ANOMALOUS COLLISION-FREE MULTIPLE IONIZATION OF ATOMS WITH INTENSE PICOSECOND ULTRAVIOLET RADIATION

T. S. Luk, H. Pummer, K. Boyer, M. Shahidi,
H. Egger, and C. K. Rhodes
Department of Physics, University of Illinois at Chicago
P.O. Box 4348, Chicago, IL 60680

ABSTRACT

Studies examining the collision-free nonlinear coupling of intense ($\sim 10^{14}$ W/cm^2) ultraviolet (193 nm) radiation to atoms spanning the range in atomic number from Z = 2 to Z = 92 are reported. The experimental data, which include the observation of U^{10+}, the production of which requires an energy transfer of $\sim$ 633 eV, a value equivalent to 99 quanta, reveal several important characteristics of these processes. Prominent features are (1) an unexpectedly strong multiphoton coupling strength resulting in multiple ionization of target atoms, (2) a strong Z-dependence of the coupling, and (3) ion charge state distributions which in some cases resemble those characteristic of Auger cascades. Conventional stepwise models of sequential ionization using standard theoretical techniques are found to be incapable of describing these results. To unify these experimental findings within the framework of a single physical picture, a mode of interaction which involves direct radiative coupling to a collective motion of an inner-shell with subsequent transfer of excitation to a corresponding outer-shell is discussed.

The availability of spectrally bright picosecond ultraviolet light sources enables the study of nonlinear coupling mechanisms in that spectral range under experimental circumstances unaffected by collisional perturbations. In this work, the results of experiments examining processes of multiple ionization of atoms with intense ($\lesssim 10^{14}$ W/cm^2) picosecond 193 nm radiation under collision-free conditions are reported.

The general physical process studied is

$$N\gamma + X \rightarrow X^{q+} + qe^- \qquad (1)$$

for which observed values of N and q range as high as 99 and 10, respectively. Of particular significance is the behavior of the amplitude for reaction (1) as a function of atomic number (Z). Accordingly, the response of several materials, spanning the range in atomic number from He (Z = 2) to U (Z = 92), has been measured. Previous work, with which we make contact in the discussion, examining similar processes involving the irradiation of Kr at 1.06 μm, has recently been described by L'Huillier et al.[1] Other preliminary studies, concerning the characteristics of Xe and Hg under intense irradiation at 193 nm have also been discussed.[2]

The experiments reported herein exhibit three salient features. These are (1) an unexpectedly strong coupling for extraordinarily high order processes, (2) a coupling strength which is dramatically enhanced at higher Z-values, and (3) a charge state distribution for the heavier materials strongly resembling that characteristic of ions formed from atomic rearrangements following the production of inner-shell vacancies.[3]

The experimental arrangement used to detect the production of the highly ionized species consists of a double focussing electrostatic energy analyzer (Comstock) operated as a time-of-flight mass spectrometer (Fig. 1). The energy analyzer is positioned in a vacuum vessel which is continuously evacuated to a

background pressure of $\sim 10^{-7}$ Torr. The materials to be investigated are introduced into the vacuum container in a controlled manner at pressures typically of $\sim 3 \times 10^{-7}$ Torr. The 193 nm ArF* laser used for irradiation[4] ($\sim$ 10 psec, $\sim$ 4 GW) is focussed by a f = 50 cm lens in front of the entrance iris of the electrostatic analyzer, producing an intensity of $\gtrsim 10^{14}$ W/cm^2 in the experimental volume. Ions formed in the focal region are collected by the analyzer with an extraction field in the range of 50-500 V/cm and subsequently detected with a microchannel plate at the exit of the electrostatic device.

Representations of the experimental results are given in Table I and Figures 2 and 3. Table I contains the normalized relative abundances of the observed ion charge states for the atomic systems studied. Fig. 2 illustrates the Z-dependence of the ion production portraying the total energies required to generate the observed ions in their electronic ground states. The inset in Fig. 2 shows a sample of typical time-of-flight ion current data for Xe. Fig. 3 displays as a histogram five representative charge state distributions illustrating the key features discussed below.

Certainly, a remarkable feature of the data is the magnitude of the total energy which can be communicated to the atomic systems. With the exception of the lighter rare gases, this energy is substantially in excess of 100 eV and culminates in a value of $\sim$ 633 eV for the production of U^{10+}, assuming the neglect of the small contributions associated with binding[5] in the parent UF_6 molecule used as the experimental material. We observe that the total energy investment of $\sim$ 633 eV needed to generate U^{10+} from the neutral atom, as estimated from available tabulations,[6-9] represents the highest value reported for a collision-free nonlinear process. In addition, it is noted that the removal of the tenth electron from uranium, which requires[7] $\sim$ 133 eV if viewed as an independent process, requires a minimum of 21 quanta. As discussed

below, the coupling implied by this scale of energy transfer at an intensity of $\sim 10^{14}$ W/cm^2 very substantially exceeds that anticipated on the basis of conventional theoretical formulations describing multiquantum ionization.

Aside from the magnitude of the observed scale of excitation energies, the shape of the envelope curve shown in Fig. 2 has significant implications. The three prominent features are (1) the general and strong tendency for increased coupling for materials heavier than argon, (2) the similarity in the response of I and Xe for which the maximum charge state observed in both cases corresponds to complete loss of the 5p-shell, and (3) a definite minimum in the energy coupled to Hg. An examination of the ionization energies[6,7] for the species involved fails to suggest any consistent picture for this behavior. For example, the removal of the fifth electron from Hg, which is not observed, requires somewhat less energy ($\sim$ 71.1 eV) than the ionization of the sixth electron from Xe ($\sim$ 71.8 eV), a process which is clearly seen. Similarly, the ionization of the second electron from He, which is not detected, requires an energy of $\sim$ 54.4 eV, a value less than that necessary to remove the fifth electron from Xe. We are led to the conclusion that some factor other than the magnitude of the ionization potentials corresponding to the different species, or equivalently, the order of the nonlinear process, governs the strength of the coupling.

An explanation based simply on the density of states is also unconvincing. A comparison of the excited state structures[10,11] for He and Ne in the relevant energy range quickly shows that the density of levels for Ne is very large in comparison to that for He, but only singly ionized species are observed for both materials.

Conversely, all three conspicuous characteristics of Fig. 2 noted above can be simultaneously understood if the shell structure of the atom is the principal physical property determining the coupling strength. The considerable

change seen in the atomic response observed between Ar and Kr strongly implicates a role for the 3d-shell which is filled in that region. A very similar variation between Ar and Kr that has been observed in the amplitude for single quantum multiple photoionization[12] has been attributed to correlation effects arising from the d-shell. A significant shell-dependent effect is also suggested by the comparative behavior of I and Xe, since complete removal of the valance 5p-shell is observed in both cases although the total energies required differ substantially. It is also known that I and Xe exhibit similar and unusually intense 4d absorptions[13,14] in the region ∿ 100 eV, strongly implicating correlated[15-17] motions in that shell. The clear minimum represented by Hg is additional testimony to the importance of the detailed nature of the atomic structure. In this case, the behavior suggests the presence of a resonance phenomenon which may result from a relationship between the binding energy characteristic of inner-shell electrons and the magnitude of the photon energy used for irradiation. Naturally, the study of materials close to Z = 80 will be necessary to establish the validity of this inference.

The most elementary mechanism that could lead to the production of the observed ionic charge states is the stepwise removal of the individual electrons by conventionally described multiphoton ionization. In this situation, a given charge state (e.g. Xe^{6+}) would require the generation of all lower charge states as its precursors thereby linking the probability for its occurrence directly to the rates of production of the lower charge states. For example, the appearance of Xe^{6+} would require a sequence of 2-, 4-, 6-, 8-, 10-, and 12-photon processes of ionization.

The probabilities for multiphoton transitions using standard perturbative approaches[18] and procedures valid in the high field limit[19] have been discussed previously for single electron systems. From these calculations, it can be shown

that, at the intensity of $\sim 10^{14}$ W/cm^2 used in these experiments, the transition rate for an N-photon process decreases very rapidly with increasing N. Indeed, an estimate shows that for N = 3, 5, 7, the relative transition probabilities scale as $1:\sim 10^{-4}:\sim 10^{-8}$. Based on these considerations, the expected charge state distributions should decrease very sharply towards higher charge states. Indeed, in this situation, the abundances of ions in charge states $q > 3$ would fall below the detection limit of the apparatus used. Consequently, it follows that the results obtained from orthodox models for multiquantum processes of this nature do not validly represent the observed experimental findings involving charge states $q > 3$. This conclusion holds for all materials studied that are heavier than Ar. Conversely, inspection of the experimental data indicates that the low Z materials, essentially up to Ar, exhibit behavior in reasonable accord with that predicted by conventional theory. Overall, this behavior can be reconciled with the presence of two different coupling mechanisms, one dominating in the low Z region and the other providing enhanced coupling in the heavier materials. From our data, the division between these two regimes appears to occur between Ar and Kr.

The form of the observed charge state distributions shown in Fig. 3 provides information on the mechanism of ion formation. In addition to the strong coupling distinguishing the heavy materials, the experimental ion distributions strongly resemble those characteristic of ions formed from atomic rearrangements arising from inner-shell vacancies. This resemblance is particularly striking[20] in comparison with ion distributions observed after x-ray ionization of the Xe and Hg N and O shells, respectively. The inference arising from this feature of the data is that an important mechanism of coupling involves a direct interaction with an inner-shell, presumably through a virtual excitation, with

subsequent transfer of excitation to a corresponding outer-shell. Interestingly, the charge state distribution shown in Fig. 3 for U possesses a double maximum. In relation to uranium, we note the recent study[21] of the very strong transition arising from 5d-f transitions in that material and the presence of an unusually narrow feature in the atomic spectrum at 10.73 nm, a wavelength that falls at an exact harmonic of the 193 nm source used in the present studies.

It is expected that nonlinear processes of the type under study should exhibit a dependence upon the wavelength of irradiation. Since Kr was examined at 1.06 μm by L'Huillier et al.[1] at the same intensity used in this work ($\sim 10^{14}$ W/cm^2), a direct comparison of ion charge distributions at 1.06 μm and 193 nm can be made. In both experiments the maximum level of ionization observed was Kr^{4+}. This comparison shows that 193 nm radiation is considerably more effective in producing the higher charge states. Relative to the abundance of Kr^+, the shorter wavelength radiation (193 nm) generated Kr^{4+} at an abundance ten-fold greater than the 1.06 μm light.

The very substantial underestimate provided by standard theoretical models of the coupling strength observed, the envelope of the Z-dependence, and the anomalous charge state distributions all conspire to support an interpretation involving an alternative mode of coupling. The enhanced and anomalous strength of the radiative interaction points to a collective response of the atom. Such a collective response, or atomic plasmon,[22] is anticipated to be favored in the outer subshells of high Z materials, namely, in shells for which the correlation energy becomes a more substantial fraction of the total electronic energy.[6,23] The coherent motion envisaged has a counterpart in nuclear matter known as the giant dipole,[24] although giant multipoles higher than the dipole are known.[25]

All aspects of the experimental findings can be unified if an important mode of nonlinear coupling involves a direct multiquantum interaction with an

atomic inner-shell which undergoes a collective response. In this picture, it would follow naturally that the shell structure of the material would be reflected as an important property governing the coupling to the radiation field. We note that collective inner-shell responses have been discussed in relation to processes of single photon ionization. More recent analyses of collective responses in atomic and molecular systems have been given by Brandt et al.,[26-28] Wendin,[15,17,29] and Amusia et al.[16,30] Furthermore, it has been found that in cases for which the electronic correlations are important, the single particle spectrum is very greatly altered, and, in certain examples, nearly eliminated and replaced by the collectively enhanced many-electron process. In this regard, the xenon $4d^{10}$ shell[29,31-34] and the lanthanides[35] have been studied extensively. The results of our current studies simply indicate a nonlinear analogue of this basic electronic mechanism. In the present experiments, the implication of the d-shell electrons seems particularly strong given the sharp change in behavior seen between Ar and Kr. Naturally, f-electrons would be expected to behave similarly, a consideration that clearly motivates study of the lanthanide sequence.

Within the framework of the physical picture described above, considerable selectivity can be expected in the population of specific states of the excited ions produced on the basis of photoelectron studies[36-39] that have been conducted on a wide range of materials. This arises since the physical coupling between the shells, the coulombic interaction, is fundamentally the same in both cases. Indeed, there is ample evidence from studies of both electron impact[40] and radiative excitation[41] of atoms that the relaxation pathways of inner-shell excited systems can readily produce inverted populations. Naturally, the presence of such selectivity is best revealed by measurements of photoelectron and photon

spectra. In addition, due to the unusually high order of the nonlinear processes observed, it is of considerable interest to investigate the role of angular momentum transfer in these interactions, an aspect that can be examined readily by the comparison of the atomic responses observed with linearly and circularly polarized radiation.

In summary, studies examining the nonlinear coupling of intense ultraviolet radiation to atomic systems, spanning the atomic number range Z = 2 to Z = 92, reveal several important characteristics of the mechanism governing this interaction. The essential findings are (1) an unexpectedly large amplitude for collision-free coupling resulting in processes involving as many as 99 quanta with an equivalent excitation energy of $\sim$ 633 eV, (2) a strong enhancement in the coupling strength for the heavy elements, (3) an ion charge state distribution resembling that produced in Auger processes, strongly implying direct coupling to inner-shell electrons, and (4) the inference, based on the atomic number dependence, the anomalous coupling strength, and the ion charge distribution, that a collective motion of d- and f-shells may play an important role in these phenomena. It is also concluded that the conventional treatment of multiquantum ionization in a model of stepwise ionization does not validly describe our experimental findings.

Support for these studies was provided by the Office of Naval Research, the Air Force Office of Scientific Research under grant no. AFOSR-79-0130, the National Science Foundation under grant no. PHY81-16636, and the Avionics Laboratory, Air Force Wright Aeronautical Laboratories, Wright Patterson Air Force Base, Ohio. In addition, fruitful discussions concerning atomic ionization energies with R. L. Carman and the skillful assistance of J. Wright and M. Scaggs in performing these studies are gratefully acknowledged.

REFERENCES

1. A. L'Huillier, L. A. Lompre, G. Mainfray, and C. Manus, Phys. Rev. Lett. 48, 1814 (1982).

2. T. S. Luk, H. Pummer, K. Boyer, M. Shahidi, H. Egger, and C. K. Rhodes, "Collision Free Generation of Highly Ionized Atomic Species with 193 nm Radiation", to be published in the Proceedings of the Topical Meeting on Excimer Lasers, Lake Tahoe, Nevada, January 10-12, 1983 (American Institute of Physics, New York, 1983).

3. M. O. Krause and T. A. Carlson, Phys. Rev. 158, 18 (1967).

4. H. Egger, T. S. Luk, K. Boyer, D. F. Muller, H. Pummer, T. Srinivasan, and C. K. Rhodes, Appl. Phys. Lett. 41, 1032 (1982).

5. G. L. DePoorter and C. K. Rofer-DePoorter, Spectrosc. Lett. 8, 521 (1975).

6. R. D. Cowan, The Theory of Atomic Structure and Spectra (University of California Press, Berkeley, 1981).

7. T. A. Carlson, C. W. Nestor, Jr., N. Wasserman, and J. D. McDowell, Atomic Data 2, 63 (1970).

8. F. T. Porter and M. S. Freedman, J. Phys. Chem. Ref. Data 7, 1267 (1978).

9. J. Bearden and A. F. Burr, Rev. Mod. Phys. 39, 125 (1967).

10. R. P. Madden and K. Codling, Astrophys. J. 141, 364 (1965); J. W. Cooper, U. Fano, and F. Prats, Phys. Rev. Lett. 10, 518 (1963); U. Fano in Photoionization and Other Probes of Many-Electron Interactions, edited by F. J. Wuilleumier (Plenum Press, New York, 1976) p. 11.

11. K. Codling, R. P. Madden, and D. L. Erderer, Phys. Rev. 155, 26 (1966).

12. J. A. R. Samson and G. N. Haddad, Phys. Rev. Lett. 33, 875 (1974); J. A. R. Samson in Photoionization and Other Probes of Many-Electron Interactions, edited by F. J. Wuilleumier (Plenum Press, New York, 1976) p. 419.

13. F. J. Comes, U. Nielsen, and W. H. E. Schwarz, J. Chem. Phys. 58, 2230 (1973).

14. D. L. Ederer, Phys. Rev. Lett. 13, 760 (1964).

15. G. Wendin, Phys. Lett. 37A, 445 (1971).

16. M. Ya. Amusia, V. K. Ivanov, and L. V. Chernysheva, Phys. Lett. 59A, 191 (1976).

17. G. Wendin in Photoionization and Other Probes of Many-Electron Interactions, edited by F. J. Wuilleumier (Plenum Press, New York, 1976) p. 61.

18. Y. Gontier and M. Trahin, Phys. Rev. 172, 83 (1968).

19. H. R. Reiss, Phys. Rev. A1, 803 (1970); ibid., Phys. Rev. Lett. 25, 1149 (1970); ibid., Phys. Rev. D4, 3533 (1971); ibid., Phys. Rev. A6, 817 (1972).

20. T. A. Carlson, W. E. Hunt, and M. O. Krause, Phys. Rev. 151, 41 (1966).

21. M. Pantelouris and J. P. Connerade, J. Phys. B16, L23 (1983).

22. F. Bloch, Z. Phys. 81, 363 (1933).

23. R. Lefebvre and C. Moser, eds., Correlation Effects in Atoms and Molecules, Adv. Chem. Phys. XIV (1969); O. Sinanoglu and K. A. Brueckner, Three Approaches to Electron Correlation in Atoms (Yale University Press, New Haven, CT, 1970); A. Hibbert, Rep. Prog. Phys. 38, 1217 (1975); A. W. Weiss, Adv. Atomic Mol. Phys. 9, 1 (1973).

24. G. C. Baldwin and G. S. Klaiber, Phys. Rev. 71, 3 (1947); ibid. 73, 1156 (1948); M. Goldhaber and E. Teller, Phys. Rev. 74, 1046 (1948).

25. Giant Multipole Resonances, edited by F. E. Bertrand (Harwood Academic Publishers, London, 1980).

26. W. Brandt and S. Lundquist, Phys. Rev. 132, 2135 (1963).

27. W. Brandt, L. Eder, and S. Lundquist, J. Quant. Spectrosc. Radiat. Transfer 7, 185 (1967); G. Wendin and M. Ohno, Phys. Scripta 14, 148 (1976).

28. W. Brandt and S. Lundquist, J. Quant. Spectrosc. Radiat. Transfer 7, 411 (1967).

29. G. Wendin, J. Phys. B3, 455 (1970); ibid., 466 (1970); ibid, B4, 1080 (1971); ibid., B5, 110 (1972); ibid., B6, 42 (1973).

30. M. Ya. Amusia, N. A. Cherepkov, and L. V. Chernysheva, Sov. Phys.-JETP 33, 90 (1971).

31. D. J. Kennedy and S. T. Manson, Phys. Rev. A5, 227 (1972).

32. J. B. West, P. R. Woodruff, K. Codling, and R. G. Houlgate, J. Phys. B9, 407 (1976).

33. G. R. Wight and M. J. Van der Wiel, J. Phys. B10, 601 (1977).

34. D. M. P. Holland, K. Codling, J. B. West, and G. V. Marr, J. Phys. B12, 2465 (1979).

35. J. P. Connerade and D. H. Tracy, J. Phys. B10, L235 (1977).

36. M. O. Krause in Synchrotron Radiation Research, edited by H. Winick and S. Donaich (Plenum Press, New York, 1980) p. 101.

37. U. Gelius, J. Electron Spectrosc. Relat. Phenom. 5, 985 (1974).

38. M. O. Krause in Photoionization and Other Probes of Many-Electron Interactions, edited by J. Wuilleumier (Plenum Press, New York, 1976) p. 133.

39. F. J. Wuilleumier in Inner-Shell and X-Ray Physics of Atoms and Solids, edited by D. J. Fabian, H. Kleinpoppen, and L. M. Watson (Plenum Press, New York, 1981).

41. W. Eberhardt, G. Kalkoffen, and C. Kunz, Phys. Rev. Lett. 41, 156 (1978); R. A. Rosenberg, M. G. White, G. Thomson, and D. A. Shirley, Phys. Rev. Lett. 43, 1384 (1979).

TABLE I. Charge state distributions (normalized to total strength) in percent.

Atom (material)*	Charge state									
	1+	2+	3+	4+	5+	6+	7+	8+	9+	10+
He	100									
Ne	100									
Ar	83	17								
Kr	68	23	8	1						
I (I_2)	14	34	19	3	0.6					
Xe	31	39	25	4	1	0.1				
Hg	61	34	5	1						
U (UF_6)	17	30	13	25	10	4	0.4	∿0.1	∿0.1	∿0.1

*Atom carried in experimentally studied material.

Figure Captions

FIG. 1. Diagram of energy and charge analyzing apparatus. The electrostatic analyzer was used as a time-of-flight instrument.

FIG. 2. Plot of the ionization energies representing the total energy transfer required for the production of different charge states as a function of atomic number (Z). The envelope curve is drawn to connect the states representing the maximum charge state observed. The inset shows a trace of typical time-of-flight data for xenon observed in these studies.

FIG. 3. Histograms of charge state distributions for Kr, I, Xe, Hg, and U.

Figure 1

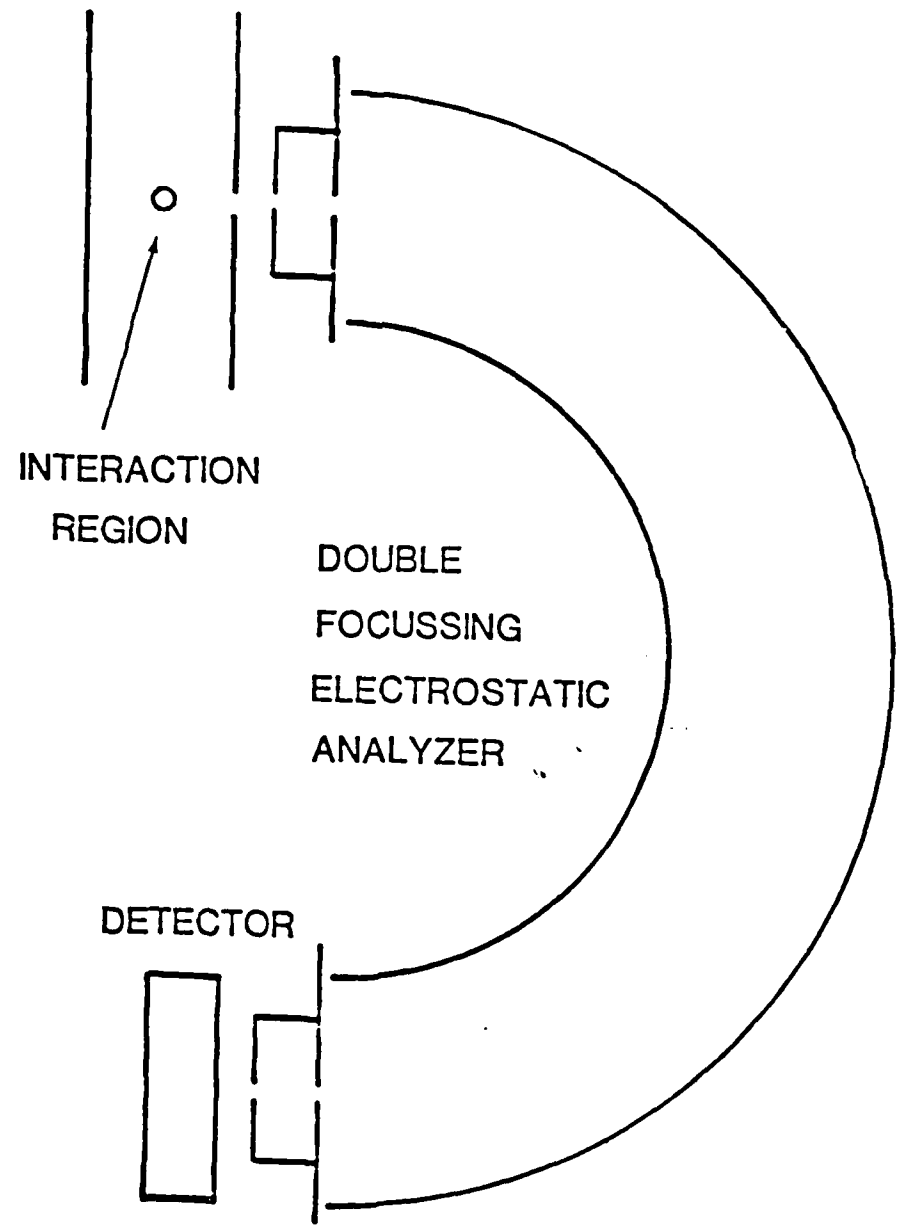
INTERACTION
REGION
DOUBLE
FOCUSSING
ELECTROSTATIC
ANALYZER
DETECTOR

Figure 2

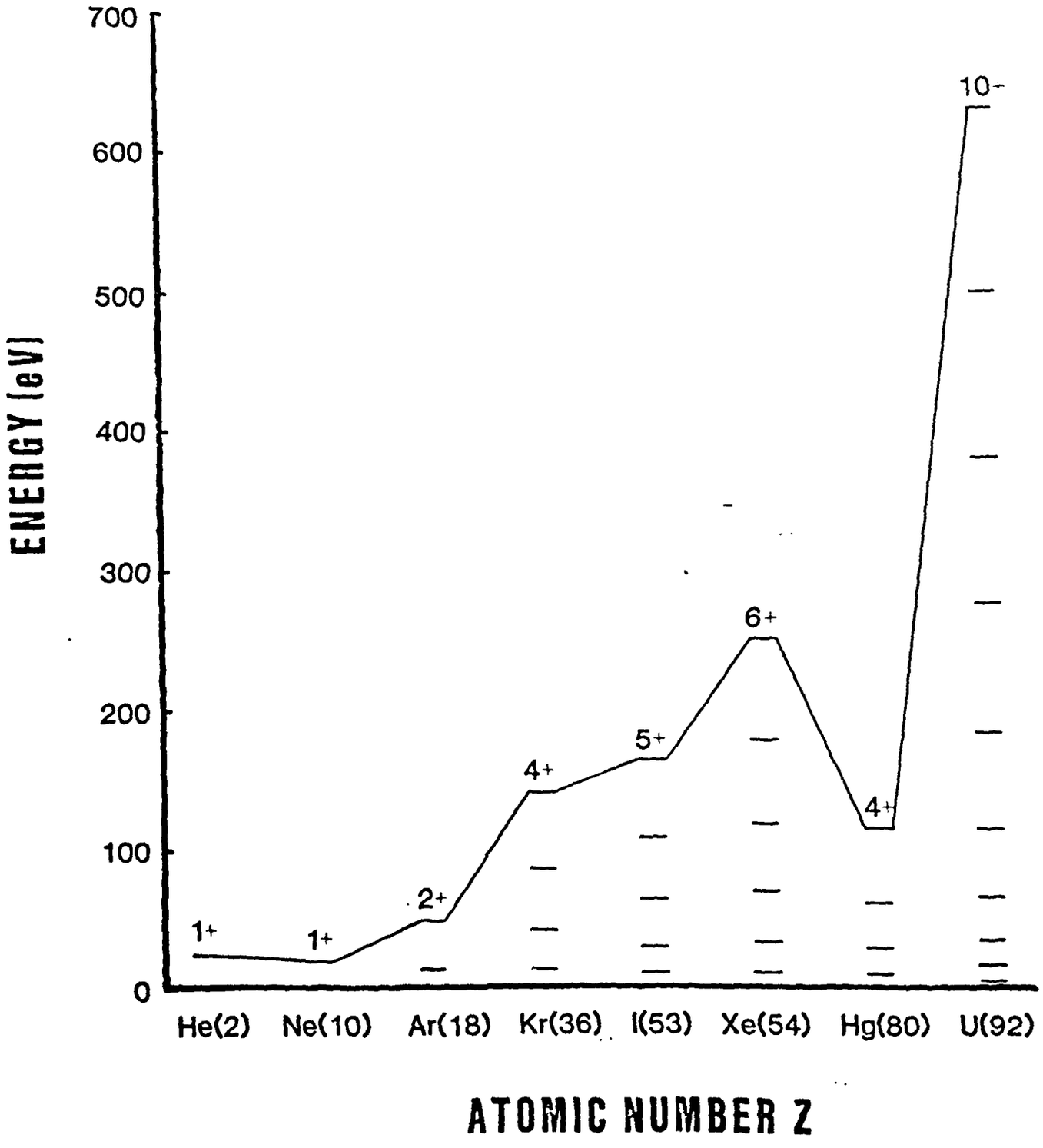
700
600
500
400
300
200
100
0
ENERGY (eV)
1+
1+
2+
4+
5+
6+
4+
10-
He(2)
Ne(10)
Ar(18)
Kr(36)
I(53)
Xe(54)
Hg(80)
U(92)
ATOMIC NUMBER Z

Figure 2 (inset)

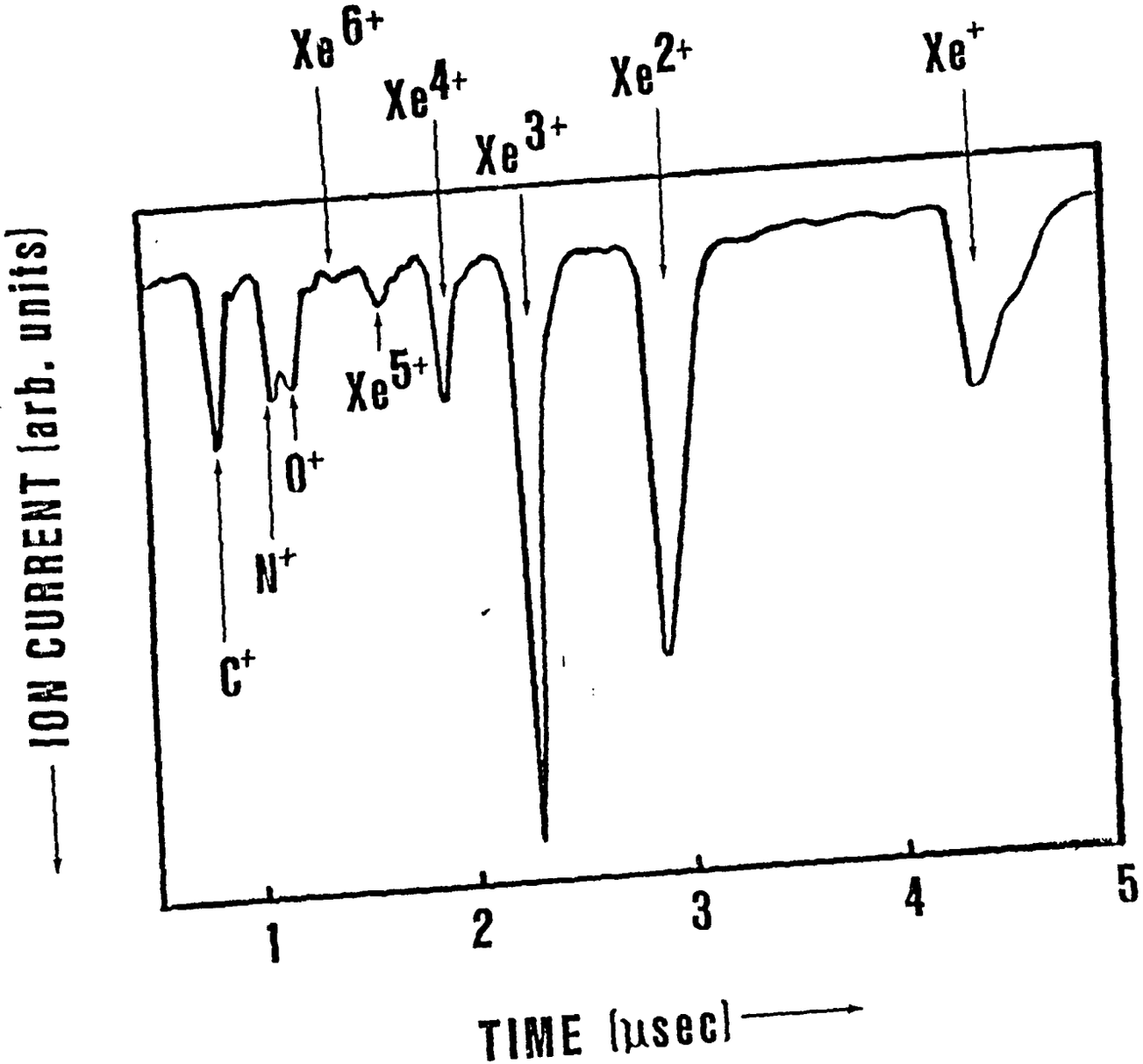

Figure 3

RELATIVE ABUNDANCE OF CHARGE STATES

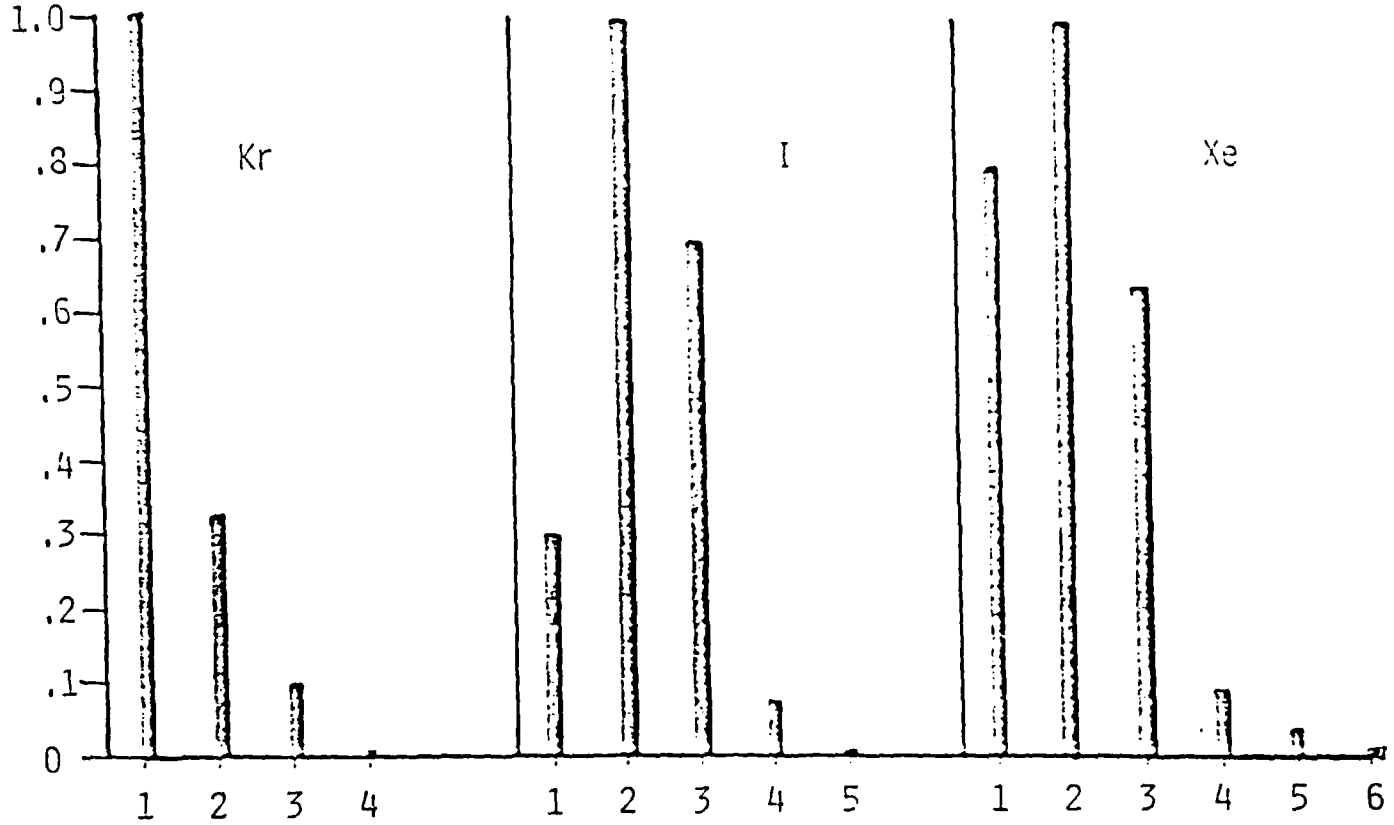

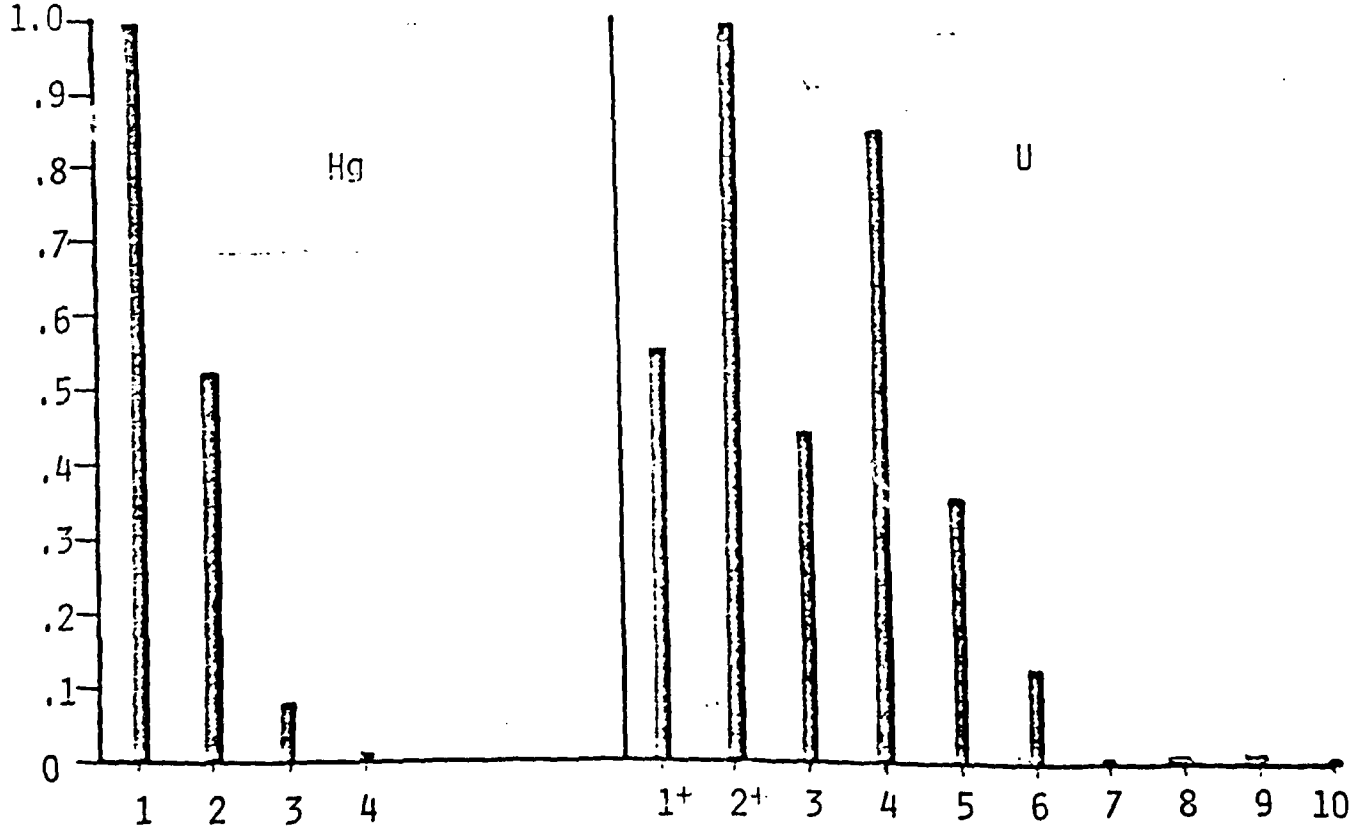

END

FILMED

9-83

DTIC